

A Naphthalene Dye: Highly Solvent-Dependent Fluorescent Sensor

Doğa Turan Kükrer

Submitted to the
Institute of Graduate Studies and Research
in partial fulfillment of the requirements for the degree of

Master of Science
in
Chemistry

Eastern Mediterranean University
March 2025
Gazimağusa, North Cyprus

Approval of the Institute of Graduate Studies and Research

Prof. Dr. Ali Hakan Ulusoy
Director

I certify that this thesis satisfies all the requirements as a thesis for the degree of Master of Science in Chemistry.

Prof. Dr. İzzet Sakallı
Chair, Department of Chemistry

We certify that we have read this thesis and that in our opinion it is fully adequate in scope and quality as a thesis for the degree of Master of Science in Chemistry.

Prof. Dr. Huriye İcil
Supervisor

Examining Committee

1. Prof. Dr. Huriye İcil

2. Prof. Dr. Nur Paşaoğluları Aydınlık

3. Assoc. Prof. Dr. Süleyman Aşır

ABSTRACT

The aim of this thesis is centred on the resynthesis, characterization, and application of a chemical derivative of naphthalene diimide. N,N'-bis(4-sulfophenyl)-1,4,5,8-naphthalene diimide (SNDI), was extensively studied and evaluated for its potential application as a chemosensor in a polar aprotic solvent. The selectivity and sensitivity of SNDI toward a range of metal cations, including Co^{2+} , Ag^+ , Cu^{2+} , Fe^{3+} , Hg^{2+} , Ca^{2+} , Mg^{2+} , Cd^{2+} , Pb^{2+} and Zn^{2+} , were investigated. FT-IR spectroscopy analysis was done to corroborate the structure of the synthesized product. This derivative of naphthalene diimide N,N'-bis(4-sulfophenyl)-1,4,5,8-naphthalene diimide (SNDI) was found to be a good candidate for chemosensor for iron and mercury ions in a polar aprotic solvent.

Keywords: naphthalene diimide, water soluble, chemosensor, polar aprotic solvent.

ÖZ

Bu tezin amacı, bir naftalin diimid türevinin yeniden sentezi, karakterizasyonu ve uygulaması üzerine odaklanmaktadır. N,N'-bis(4-sülfenil)-1,4,5,8-naftalin diimid (SNDI), polar aprotik bir çözücü içinde kemosensör olarak potansiyel uygulaması açısından kapsamlı bir şekilde incelenmiş ve değerlendirilmiştir. SNDI'nin Co^{2+} , Ag^+ , Cu^{2+} , Fe^{3+} , Hg^{2+} , Ca^{2+} , Mg^{2+} , Cd^{2+} , Pb^{2+} ve Zn^{2+} gibi bir dizi metal katyonuna karşı seçiciliği ve duyarlılığı araştırılmıştır. Sentezlenen ürünün yapısını doğrulamak için FT-IR spektroskopi analizi yapılmıştır. Bu naftalin diimid türevi olan N,N'-bis(4-sülfenil)-1,4,5,8-naftalin diimid (SNDI), polar aprotik bir çözücüde demir ve civa iyonları için iyi bir kemosensör adayı olarak bulunmuştur.

Anahtar Kelimeler: naftalin diimid, polar aprotik çözücü, suda çözülen, kemosensör

ACKNOWLEDGEMENT

I would like to thank my supervisor Prof. Dr. Huriye İcil for her endless support and incredible supervision that she provided for me through my master's degree journey. Her wisdom, insight and approach to research and science has been truly an inspiration. She provided me with unwavering support, and constructive feedback throughout every stage of this research. She is more than a supervisor, more than a professor, more than a doctor. She is a mentor, an inspiring individual and a mother-figure.

I would like to extend my sincere thanks to my jury members Prof. Dr. Nur Paşaoğulları Aydınlık and Assoc. Prof. Dr. Süleyman Aşır for their contributions to my thesis journey.

I am grateful for the precious friends I made throughout my journey. Spending my laboratory hours with Arwa, Pelin, Meltem and Seval were nothing short of heart-warming. With their infinite support and friendship, they have made this experience unforgettable.

Last but not least, I would like to display my deepest gratitude to my family. Without my partner, father, mother, sister and uncle, I would not be the person who I am today. I will be forever thankful for their boundless support and immeasurable love. As for my little boy, Noa, seeing his face every single day has made me push through every single obstacle throughout this journey.

TABLE OF CONTENTS

ABSTRACT	iii
ÖZ	iv
ACKNOWLEDGEMENT	v
LIST OF TABLES	viii
LIST OF FIGURES	ix
LIST OF ABBREVIATIONS	xii
1 INTRODUCTION	1
1.1 Diimide Groups & Naphthalene Diimides.....	1
1.2 Structure of Naphthalene Diimide.....	1
1.3 Properties and Applications of Naphthalene Diimides.....	3
1.4 Aim of the Study.....	6
2 THEORETICAL.....	8
2.1 Chemosensors	8
2.2 Heavy Metals	10
2.3 Naphthalene Diimides as Chemosensors	11
3 EXPERIMENTAL	13
3.1 Materials	13
3.2 Instruments.....	13
3.3 Procedure of N,N'-bis(4-sulfohenyl)-1,4,5,8-napthalene diimide (SNDI) Synthesis	13
3.4 Mechanism of the Reaction.....	15
3.5 UV-Vis Absorption and Emission Spectroscopy Analysis.....	17
4 DATA AND CALCULATIONS.....	18

4.1 Molar Calculations	18
5 RESULTS AND DISCUSSION	40
5.1 Synthesis of SNDI	40
5.2 FT-IR Spectra Analysis of SNDI.....	40
5.3 Solubility of SNDI.....	40
5.4 UV-Vis Absorption and Emission Spectra Analysis of SNDI.....	41
5.5 UV-Vis Absorption and Emission Spectra Analysis of SNDI with Metal Cations	42
6 CONCLUSION.....	45
REFERENCES	46

LIST OF TABLES

Table 5.1: Solubility table of SNDI in several solvents.....	41
--	----

LIST OF FIGURES

Figure 1.1: Structure of Naphthalene Diimide (NDI).....	2
Figure 1.2: Structure of SNDI.	7
Figure 3.1: Synthesis schematic of N,N'-bis(4-sulfophenyl)-1,4,5,8-naphthalene diimide (SNDI).....	14
Figure 3.2: Nucleophilic attack from 4-aminobenzene sulfonic acid to NDA.....	15
Figure 3.3: Intermolecular proton transfer of newly formed SNDI.....	16
Figure 3.4: Proton transfer from SNDI to isoquinoline as well as intermolecular proton transfer to close the ring structure of SNDI.	16
Figure 3.5: Proton transfer between isoquinoline and hydroxide ion.....	17
Figure 4.1: FT-IR spectrum of 1,4,5,8-Naphthalenetetracarboxylic dianhydride (NDA), KBr pellet.	19
Figure 4.2: FT-IR spectrum of 4-aminobenzene sulfonic acid, KBr pellet.....	20
Figure 4.3: FT-IR spectrum of N, N'-bis(4-sulfophenyl)-1,4,5,8-naphthalene diimide (SNDI).....	21
Figure 4.4: UV-vis absorption spectra of SNDI in the presence of metal ions.	22
Figure 4.5: UV-vis emission spectra of SNDI in DMF at excitation wavelength of 225 nm (top) 360 nm (bottom).....	23
Figure 4.6: UV-vis emission spectra of 1.67×10^{-6} M Fe^{+3} in DMF at excitation wavelength of 225 nm (top) 360 nm (bottom).	24
Figure 4.7: UV-vis emission spectra of SNDI with 1.67×10^{-6} M Fe^{+3} in DMF at excitation wavelength of 225 nm (top) 360 nm (bottom).	25
Figure 4.8: UV-vis emission spectra of 1.67×10^{-6} M Hg^{+2} in DMF at excitation wavelength of 225 nm (top) 360 nm (bottom).	26

Figure 4.9: UV-vis emission spectra of 1.67×10^{-6} M Hg^{+2} in DMF at excitation wavelength of 225 nm (top) 360 nm (bottom).	27
Figure 4.10: UV-vis emission spectra of SNDI in DMF in the presence of 3.33×10^{-7} M metal ions at excitation wavelength 225 nm.	28
Figure 4.11: UV-vis emission spectra of SNDI in DMF in the presence of 3.33×10^{-7} M metal ions at excitation wavelength 360 nm.	29
Figure 4.12: UV-vis emission spectra of SNDI in DMF in the presence of 1.67×10^{-6} M metal ions at excitation wavelength 225 nm.	30
Figure 4.13: UV-vis emission spectra of SNDI in DMF in the presence of 1.67×10^{-6} M metal ions at excitation wavelength 360 nm.	31
Figure 4.14: UV-vis emission spectra of SNDI in the presence of 1.67×10^{-6} M Fe^{+3} solution and DMF at excitation wavelength 225 nm.	32
Figure 4.15: UV-vis emission spectra of SNDI in the presence of 1.67×10^{-6} M Fe^{+3} solution and DMF at excitation wavelength 360 nm.	33
Figure 4.16: UV-vis emission spectra of SNDI in various concentrations of Fe^{+3} in DMF at excitation wavelength 225 nm.	34
Figure 4.17: UV-vis emission spectra of SNDI in various concentrations of Fe^{+3} in DMF at excitation wavelength 360 nm.	35
Figure 4.18: UV-vis emission spectra of SNDI in the presence of 1.67×10^{-6} M Hg^{+2} solution and DMF at excitation wavelength 225 nm.	36
Figure 4.19: UV-vis emission spectra of SNDI in the presence of 1.67×10^{-6} M Hg^{+2} solution and DMF at excitation wavelength 360 nm.	37
Figure 4.20: UV-vis emission spectra of SNDI in various concentrations of Hg^{+2} in DMF at excitation wavelength 225 nm.	38

Figure 4.21: UV-vis emission spectra of SNDI in various concentrations of Hg^{+2} in DMF at excitation wavelength 360 nm.....39

LIST OF ABBREVIATIONS

AAS	Atomic Absorption Spectroscopy
ACE	Acetone
ADI	Arylene Diimide
CHL	Chloroform
CH ₃ CN	Acetonitrile
CNDI	Core Substituted NDI
CT	Charge Transfer
°C	Degree Celsius
cm	Centimetre
DNA	Deoxyribonucleic Acid
DMF	N,N'-dimethylformamide
DMSO	Dimethyl Sulfoxide
FET	Field-Effect Transistor
FT-IR	Fourier Transform Infrared Spectroscopy
g	Grams
HEPES	4-(2-Hydroxyethyl)piperazine-1-ethanesulfonic Acid Sodium Salt
ICP	Inductively Coupled Plasma
IR	Infrared
KBr	Potassium Bromide
M	Concentration
NDA	1,4,5,8-Naphthalene Tetracarboxylic Dianhydride
NDI	Naphthalene Diimide
nm	Nanometre

OFET	Organic Field-Effect Transistor
PDI	Perylene Diimide
PMDI	Pyromellitic Diimide
PYR	Pyridine
RDI	Rylene Diimide
SNDI	N,N'-bis(4-sulfophenyl)-1,4,5,8-Naphthalene Diimide
THF	Tetrahydrofuran
TLC	Thin Layer Chromatography
UV	Ultraviolet
UV-vis	Ultraviolet-visible

Chapter 1

INTRODUCTION

1.1 Diimide Groups & Naphthalene Diimides

Arylene diimides (ADIs) are a class of redox-active aromatic compounds known for their superb chemical, photochemical and thermal stabilities. Exceptional features of these compounds have shown to be highly advantageous across different disciplines, such as materials science, biological chemistry and supramolecular chemistry. Among the various types of ADIs, naphthalene diimides (NDIs), perylene diimides (PDIs) and pyromellitic diimides (PMDIs) are the most extensively studied and recognized [1]. NDI is the smallest unit of the rylene diimide class, which also includes the well-studied PDI. NDIs are mostly regarded for their high electron affinity, superior charge carrier mobility, and distinguished oxidative and thermal stability. These qualities make NDIs magnificent choices for use in organic electronics, solar panels, and flexible displays [2]. NDIs are part of ADIs due to them belonging to the broader class of aromatic compounds with diimide functional groups. However, NDIs are also considered the smallest members of the rylene diimides (RDI) family, which includes larger homologues like perylene diimides (PDIs) [1-2].

1.2 Structure of Naphthalene Diimide

The NDI structure consists of a naphthalene core with two electron-acceptor imide groups attached at its four α -positions. The nitrogen atoms of these imide groups can be further functionalized with a wide range of alkyl or aryl substituents [3]. At positions 1, 4, 5, and 8, it has two electron-withdrawing imide groups attached, which

reduce the charge density on the naphthalene core. A highly acidic π -surface is caused by this phenomenon. These features make NDI a versatile building block for making complex supramolecular structures. Naphthalene core plays a vital role in stabilising these structures through a set of interactions, including van der Waals forces, π - π stacking and charge transfer (CT) interactions. Furthermore, hydrogen bonding can occur with aromatic C–H and C=O groups, and the imide groups can take part in metal coordination [1][3]. Chemical structure of NDI is shown in Figure 1.1.

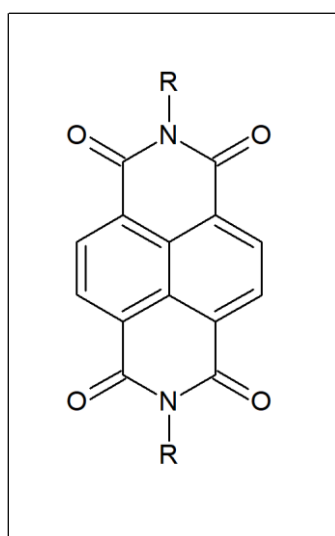


Figure 1.1: Structure of Naphthalene Diimide (NDI).

NDIs are characterized by a lipophilic naphthalene core combined with four polar carbonyl functional groups. Depending on the variety of imide substituents, the combination of the lipophilic core with the carbonyl functional groups makes NDIs soluble in polar aprotic solvents such as acetonitrile, DMF, and DMSO as well as low-polarity solvents like toluene, dichloromethane, and chloroform. NDI molecules have a tendency to stack together due to their flat, aromatic structure, which are further stabilised by π - π interactions [4].

1.3 Properties and Applications of Naphthalene Diimides

NDIs have been under the spotlight in recent years because of their unique features. They are highly versatile due to their flat, planar structure and electron-deficient nature, as well as their strong visible light absorption, high quantum efficiency, and excellent redox activity, which are photochemical and electrochemical properties. Moreover, they are quite popular in applications such as sensors, light harvesting, photocatalysis and self-assembly structures due to their easily modifiable structure [5].

NDIs are highly durable aromatic molecules with a sturdy, neutral, and planar core. They also possess unique chemical and physical properties. They are prominent as electron-deficient acceptors and are often utilised in creating charge transfer complexes by pairing with various electron-rich donors, such as derivatives of pyrene and dioxynaphthalene [6].

NDIs have proven to be quite important in biomedicine and cancer research. They exhibit properties such as DNA intercalation, antiviral, antimicrobial and anticarcinogenic properties [7]. For example, it was discovered that an NDI intercalator, when attached to the C4 amine of a methylated cytosine base, can act as a long-range DNA photooxidant [8]. Furthermore, several water-soluble NDI derivatives display a specific type of interaction with DNA, called threading. This specific interaction enables NDIs to be designed as molecular probes [9]. On the other hand, coordination complexes of NDIs show great potential in applications like intercalators and luminescent probes. NDIs can be reduced through chemical or electrochemical methods with ease, forming stable radical anions. This makes them excellent electron acceptors, which is why they are widely used in artificial

photosynthetic systems for solar energy conversion, as well as in the design of supramolecular switches like catenanes and rotaxanes. Additionally, NDIs have a tendency to form n-type semiconductor materials with high electron mobility, making them more favourable than p-type materials in many cases [10].

NDIs have gathered immense attention due to this n-type forming tendency. Their ability to self-organize and integrate into larger, multicomponent assemblies through intercalation is also a critical factor in NDIs popularity. Their versatility emerges from the functionalization of their structure. Modifying the diimide nitrogens or substituting the naphthalene core allows for a wide range of absorption and emission properties. For instance, adding aromatic groups to the diimide nitrogens results in non-fluorescent or weakly fluorescent compounds, while alkyl substitutions typically produce the characteristic white-blue fluorescence of NDIs [4]. NDIs are widely used in n-type semiconductors, field-effect transistors (FETs), and solar energy conversion technologies, thanks to their photo-induced electron transfer properties. Their ability to form complex structures through interactions like π -stacking, hydrogen bonding, and van der Waals forces also makes them versatile in supramolecular chemistry [11]. This adaptability has made NDIs increasingly popular since the mid-20th century, following the pioneering research conducted by Vollmann and his team in the early 1930s. Their ability to be tailored for diverse applications continues to solidify their place in advanced material science [4] [12].

Meanwhile, core substituted NDIs (cNDIs) are emerging as a distinct class due to their enhanced conductivity, and unique photophysical properties compared to the core unsubstituted NDIs. cNDIs are colourless compounds with high extinction coefficient at the boundary of UV-A and visible light [13]. They demonstrate a potential in

synthesizing vibrant, conductive, and functional compounds with photophysical properties that are significantly different from those of their unsubstituted counterparts. By modifying NDIs to obtain cNDIs, researchers have developed a wide range of useful materials. These cNDIs have been used in applications such as dyes, pigments, sensors, molecular aggregates, and both n-type and p-type organic semiconductors [12]. Core substitution in NDIs has led to significant advancements in tuning their optical and redox properties. This breakthrough has greatly expanded the potential applications of various dyes, opening new possibilities for their use [14].

A key feature that NDI possess, is that the modification of nitrogen atoms usually does not affect the optical or electrochemical properties significantly. Instead, they significantly influence solubility, crystallinity, and the aggregation behaviour of the molecules [15]. This happens because there is a node in the wavefunction at the imide nitrogen, which effectively shields the NDI unit from the inductive or mesomeric effects of the substituents. On the other hand, the two N-substituents play a major role in determining how small-molecule NDI derivatives pack together in the solid state. This packing can have a massive impact on performance ranging from excellent transistor behaviour to complete inactivity in organic field-effect transistors (OFETs) [16].

NDIs are intensively applied as chemosensors and biosensors in the industry. NDIs are excellent candidates for sensors because they are small, easy to modify, and have decent solubility in various solvents. Their fluorescent properties can also be fine-tuned, making them versatile for different applications. While NDIs themselves do not emit much light, cNDIs can fluoresce, especially when electron-donating groups like alkyl amines are added. Adjusting the substituents on a cNDI can have a substantial

impact on its absorbance and fluorescence. These changes are easy to measure, making cNDIs ideal for creating highly effective sensors [17]. Unmodified NDI dyes generally have low fluorescence quantum yields due to their strong electron-deficient nature. However, modifications can significantly enhance fluorescence quantum yield. Pure NDI cores typically exhibit fluorescence in the blue-green region rather than across the entire visible spectrum from green to red and near IR. To achieve red or near IR emission, chemical modifications (core expansion, donor-acceptor systems, or introduction of heavy atoms) are usually necessary. This near-IR capability is especially valuable for biological applications, as it allows the signal to penetrate tissues, enhances detection, and minimizes the risk of photo-damage [18].

1.4 Aim of the Study

Aim of this thesis is to resynthesize, purify and fully characterize a water soluble and N-modified NDI derivative which is previously synthesized by Rajab [19], N, N'-bis(4-sulfophenyl)-1,4,5,8-naphthalene diimide (SNDI). Characterization of SNDI was achieved through techniques including Fourier Transform Infrared Spectroscopy (FT-IR) and Fluorescence Spectroscopy. Furthermore, SNDI was examined for its potential application as a chemosensor in detecting a range of heavy metal cations. The interactions between SNDI and several metal ions, which are, Co^{2+} , Ag^+ , Cu^{2+} , Fe^{3+} , Hg^{2+} , Ca^{2+} , Mg^{2+} , Cd^{2+} , Pb^{2+} , and Zn^{2+} , were analysed using UV-vis absorption and emission spectroscopy techniques. Figure 1.2 shows the structure of the synthesized SNDI.

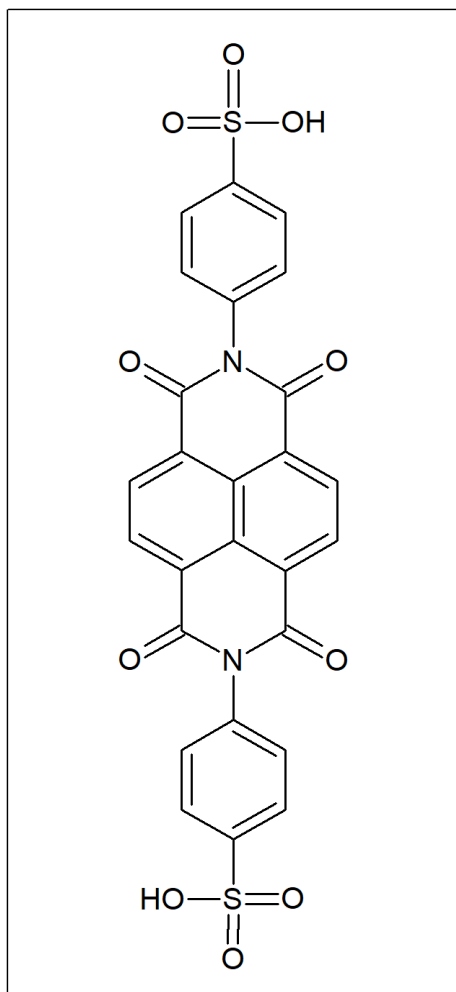


Figure 1.2: Structure of SNDI.

Chapter 2

THEORETICAL

2.1 Chemosensors

Chemosensors have gained significant interest in the scientific community because of their wide-ranging potential uses in fields like chemistry, biology, medicine, environmental science, and even in the industry [20]. The term "chemosensor" describes a synthetic molecule designed to detect the presence of energy or matter. These sensors are widely recognized as tools that selectively and often reversibly bind to specific analytes, changing properties like fluorescence, colour, or redox potential [21]. A chemosensor can also be described as "a sensory receptor that converts a chemical signal into an action potential" [22]. Specifically, when the receptor is made up of chemically synthesized molecules, the resulting sensor is generally referred to as a chemosensor. On the other hand, if the receptor is based on biological components, such as natural macromolecules like protein, nucleic acids, or peptides, the sensor is more accurately called a biosensor. A biosensor can be described as essentially a chemosensor equipped with a biological receptor [23]. In other words, a biosensor is simply a specialized type of chemosensor that has a bioreceptor.

A high-quality chemosensor is defined by its sensitivity and selectivity toward a specific analyte. Key properties such as ion affinity, solubility, strong fluorescence, or visible colour changes are highly desirable and play a critical role in the design of effective chemosensors [24]. The functional interactions that underpin chemosensor

performance include hydrophobic effects, van der Waals forces, ionic and hydrogen-bond interactions, metal chelation, covalent bonding and π -cation interactions, among others. The chemosensor's particular design ultimately dictates which of these interactions will be activated during the sensing process, enabling the detection of the target analyte [24-25].

Chemosensors can be categorized into various types based on their operating principles. Common types include electrical sensors and optical sensors, which are colorimetric and fluorescence sensors [26]. In the last few decades, optical chemosensors have become especially popular in fields like environmental science, molecular biology, and medicine because of their exceptional sensitivity and ability to provide real-time monitoring [27]. In principle, optical signalling chemosensors are developed based on utilizing the photophysical changes that occur when different types of analytes, including metal cations, anions, small biological scaffolds and neutral molecules, are detected using the supramolecular host-guest chemistry [28].

The development of colorimetric chemosensors for selective sensing of anions and cations both chemically and biologically has gathered significant attention due to their high selectivity, sensitivity, as well as “naked eye” detection, eliminating the need for expensive instruments [26-28].

Fluorescent chemosensors are chemical species designed with special fluorescent properties that allow them to interact with specific analytes. This interaction is observed through changes that are detectable such as thermal, magnetic, electrical, electronic, or most frequently, optical shifts [29]. In 1867, Goppelsroder created the first fluorescent chemosensor and used it to detect Al^{3+} ions. Since then, fluorescence

chemosensors have been widely used for precise measurements of different analytes in solution in fields ranging from analytical chemistry to physiology [30]. The fluorescence detection method for metal ions has garnered significant interest among researchers worldwide. This approach is based on the specific interactions between fluorescent probes and target analytes, which either enhance or quench fluorescence intensity. To date, a wide range of fluorescent probes, including small organic molecules, carbon quantum dots, covalent organic frameworks, metal nanoparticles, and dye molecules, have been developed and successfully applied for the detection of metal ions, demonstrating remarkable performance [31]. The fluorescence detection method offers several advantages, such as rapid response times, cost-effectiveness, ease of operation, and high sensitivity [32]. Fluorescent chemosensors have emerged as a promising tool for the practical detection of metal ions. Traditional analytical techniques, such as inductively coupled plasma (ICP), electrochemical methods and atomic absorption spectroscopy (AAS), often require substantial sample volumes, expensive equipment, and complex procedures for analysis. Given these limitations, fluorescent chemosensors have become a viable alternative, enabling the broad detection of metal ions, anions, protons, and small molecules with the added advantage of on-site and real-time observation [32-34].

2.2 Heavy Metals

Heavy metals rank among the most dangerous pollutants present in wastewater, air, and soil [35]. The rapid pace of industrial development and urbanization has led to widespread environmental pollution on a global scale. Among these pollutants, heavy metals are particularly pervasive. While some heavy metals are essential for industrial applications, their release into the environment poses significant risks. These metals can enter the human body through the food chain, ultimately becoming a serious threat

to human health [36]. Heavy metals are generally defined as metals with a density greater than 5 g/cm³. While certain trace elements, such as Copper (Cu), manganese (Mn), and zinc (Zn), are crucial for various biological functions, most heavy metals including nickel (Ni), mercury (Hg), cobalt (Co), cadmium (Cd), arsenic (As), chromium (Cr), and lead (Pb) are non-essential and do not contribute to vital biological processes. Although heavy metals are naturally present in soils in trace amounts, their excessive accumulation can degrade soil quality and negatively impact plant life on the surface [37].

Mercury (Hg) is highly toxic and poses significant dangers to biological systems. Even trace amounts of mercury ions in drinking water can have severe, potentially lethal effects on human health, primarily due to their ability to cause neurological damage. Mercury exposure has been linked to numerous chronic diseases, including neurological disorders, Hunter-Russell syndrome, leukaemia, and Minamata disease [38]. Mercury can exist in various forms, including metallic species, as well as organic and inorganic compounds. Among these, organomercury compounds are notably more toxic than inorganic mercury salts. Mercuric (Hg²⁺) ions are commonly found in the form of mercuric salts or as coordinated complexes with elements such as oxygen, sulphur, and chlorine [39].

2.3 Naphthalene Diimides as Chemosensors

Arylene diimides, particularly naphthalene diimides (NDIs) are n-type organic semiconductors renowned for their exceptional photophysical properties. These self-assembled π -system moieties, with their superior photophysical characteristics, are highly versatile and find applications in a wide range of fields, including dye lasers, organic electronics, and as fluorogenic probes for chemical/biological sensing and

imaging [40]. Naphthalene diimide (NDI) has found extensive use in the fabrication of supramolecular self-assembled nanomaterials and as a key component in n-type semiconductors. Additionally, NDI derivatives have demonstrated their potential as effective probes for the colorimetric sensing of metal ions [41]. Naphthalene diimides, which can be classified as fluorescent organic molecules, are highly appealing candidates for fluorescent sensors due to their exceptional optical, thermal, and electrochemical properties. However, water solubility stands out as a critical factor for the practical application of fluorescence sensors. In particular, there is a strong emphasis on designing chemosensors that are easy to synthesize, cost-effective, water-soluble, and exhibit high sensitivity and selectivity for the detection of heavy metal ions in aqueous environments [42].

In contrast to previously reported chemosensors, the synthesis of NDI derivatives does not require costly raw materials [43]. A significant advantage using NDI derivatives lies in the ability to tailor their properties by introducing various substituents onto the core section of the naphthalene, which can improve their water solubility. Derivatives of NDI featuring π - π stacking sites and hydrophilic groups show great promise as effective chemosensors for detecting and removing heavy metal cations in aqueous systems. In NDI-based chemosensors, the NDI segment functions as the site for π - π stacking, while imide position substituents serve as hydrophilic groups which facilitate interactions with heavy metal cations [44].

Chapter 3

EXPERIMENTAL

3.1 Materials

Every chemical used in this research got obtained from private enterprises, without further purifying procedure. All the solvents used in the synthesis process were refined using distillation. Spectroscopic-grade solvents were used without further purifying procedure. 1,4,5,8-Naphthalene tetracarboxylic dianhydride, isoquinoline, zinc acetate, 4-aminobenzenesulfonic acid, perchlorate salts of Co^{2+} , Ag^+ , Cu^{2+} , Fe^{3+} , Hg^{2+} , Ca^{2+} , Mg^{2+} , Cd^{2+} , Pb^{2+} , Zn^{2+} were obtained from Sigma Aldrich.

3.2 Instruments

Thin layer chromatography (TLC) using Merk silica gel aluminium coated films was used to track the progression of the reactions, and the results were observed under a UV lamp. Using KBr pellets and a JASCO FT-IR spectrophotometer, infrared spectra were obtained. A Varian-Cary 100 spectrophotometer was used to record all UV-vis absorption spectroscopy measurements. With the use of quartz cells, a Varian Cary Eclipse spectrophotometer was used for all emission spectroscopy measurements.

3.3 Procedure of N,N'-bis(4-sulfophenyl)-1,4,5,8-naphthalene diimide (SNDI) Synthesis

The synthesis procedure was carried out through a condensation reaction, utilizing 1.0 g of 1,4,5,8-naphthalene tetracarboxylic dianhydride, 2.6 g of 4-aminobenzene sulfonic acid, and 0.8 g of zinc acetate as the catalyst. This reaction was carried out in

a dried solvent of 10 ml isoquinoline under an inert nitrogen atmosphere. The solution was heated in stages: 80 °C for 2 hours, 100 °C for 3 hours, 120 °C for 1 hour, 140 °C for 6 hours, 160 °C for 7 hours, 180 °C for 2 hour and 200 °C for 2 hours. After cooling, the solution was added to 250 ml of cold acetone, causing a precipitate to form. This precipitate was filtered and dried under vacuum. To remove any high-boiling-point solvents, unreacted amine and remaining catalyst, the crude product was purified using the Soxhlet extraction method with acetone for one week. The final product, a pale-yellow crystal of SNDI, was obtained through recrystallization from an acetone/water mixture. Synthesis schematic of SNDI is shown in figure 3.1.

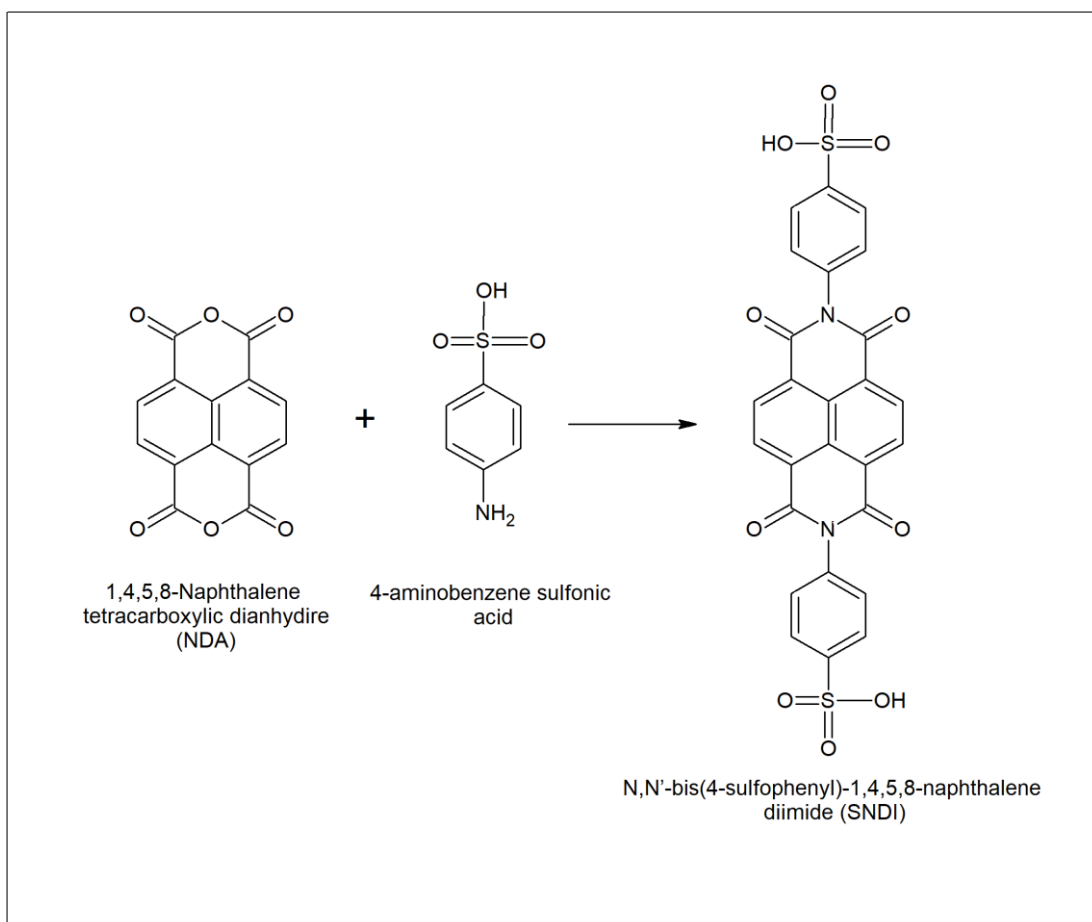


Figure 3.1: Synthesis schematic of N,N'-bis(4-sulfophenyl)-1,4,5,8-naphthalene diimide (SNDI).

Yield: 88% (1.90g) **Colour:** Pale yellow.

3.4 Mechanism of the Reaction

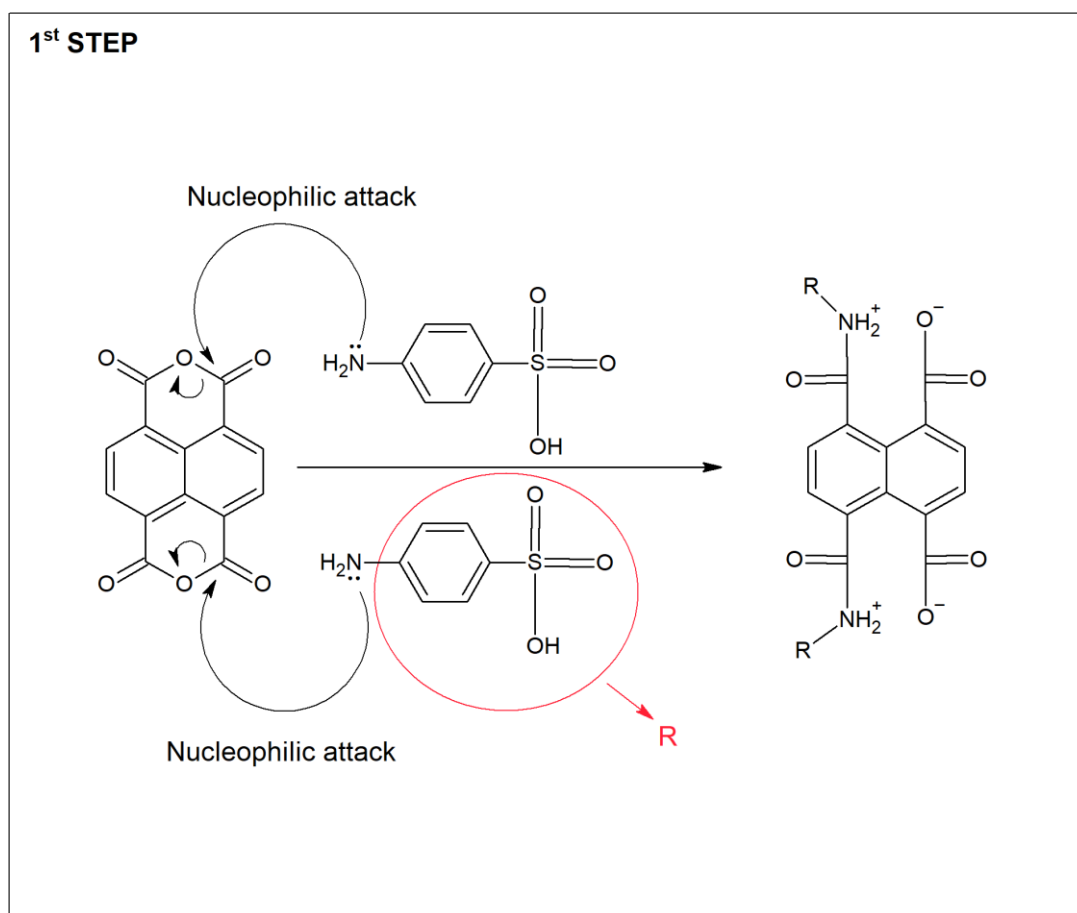


Figure 3.2: Nucleophilic attack from 4-aminobenzene sulfonic acid to NDA.

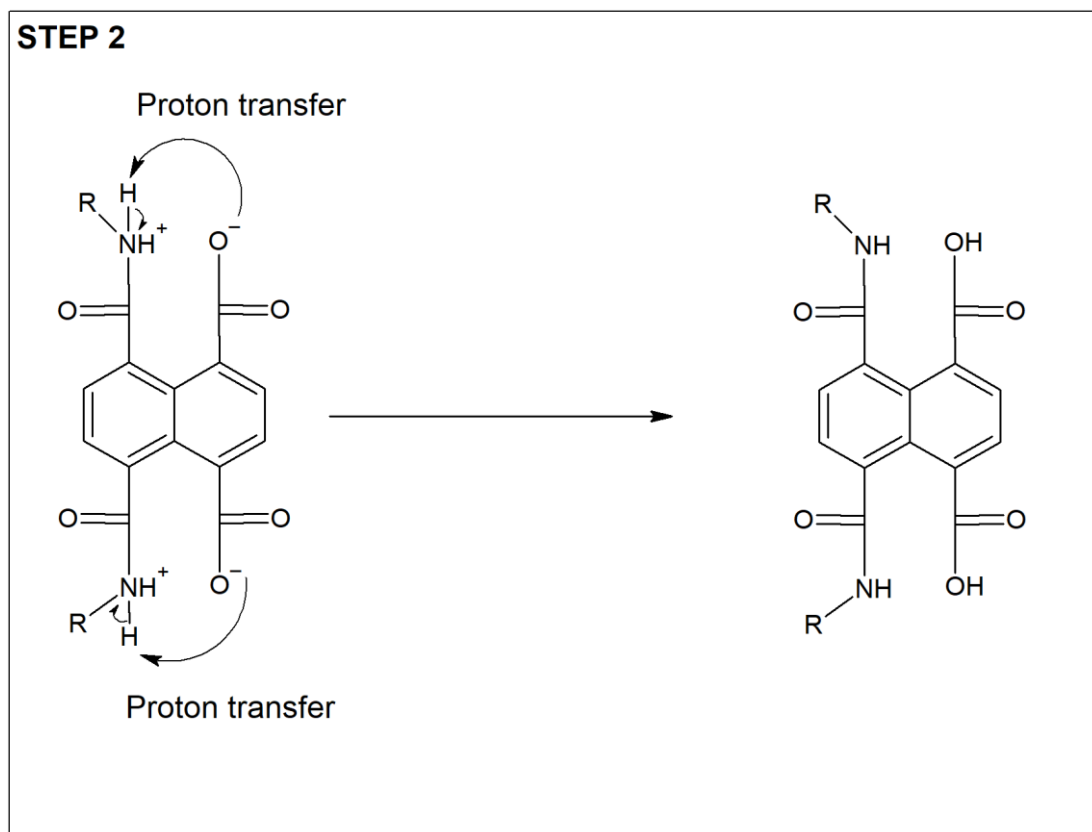


Figure 3.3: Intermolecular proton transfer of newly formed SNDI.

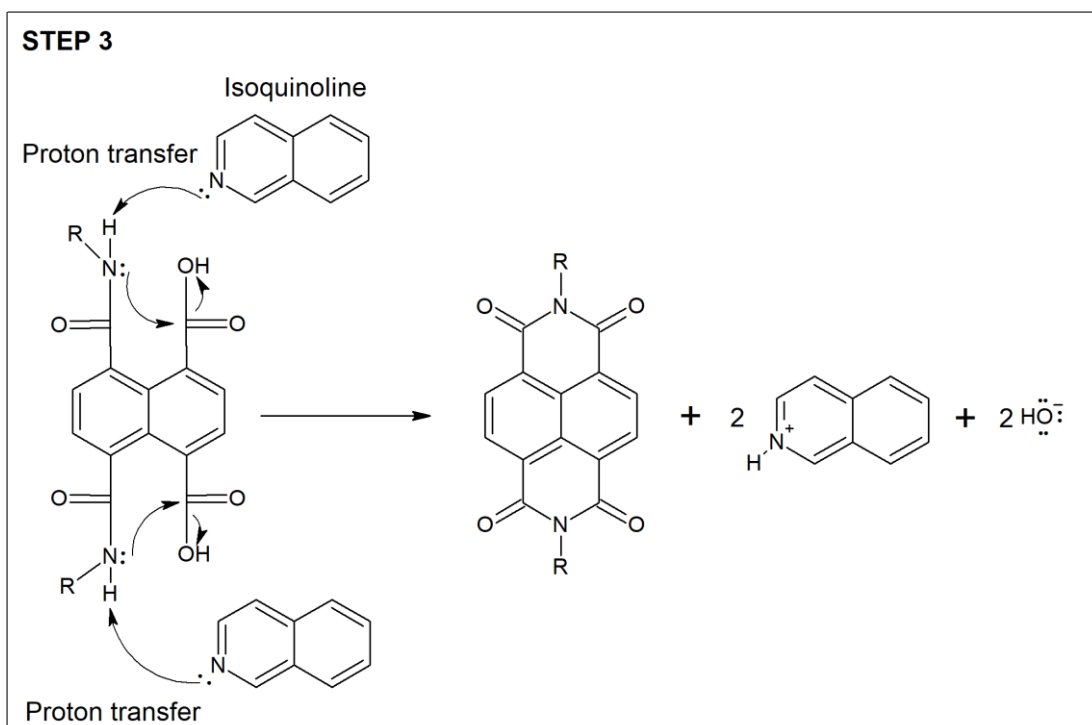


Figure 3.4: Proton transfer from SNDI to isoquinoline as well as intermolecular proton transfer to close the ring structure of SNDI.

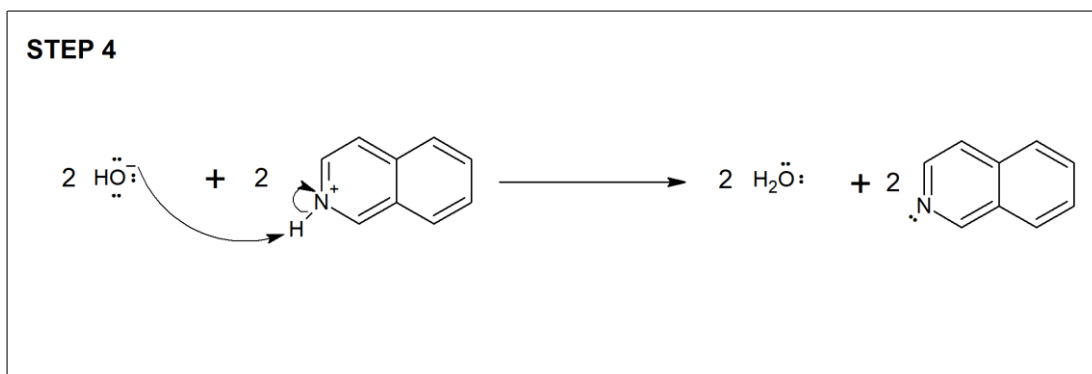


Figure 3.5 Proton transfer between isoquinoline and hydroxide ion.

3.5 UV-Vis Absorption and Emission Spectroscopy Analysis

First, without the addition of any metal cations, UV-visible and fluorescence spectra of 1.0×10^{-5} M SNDI were collected at excitation wavelengths of 225 and 360 nm. Following the introduction of 10 metal solutions of Co^{2+} , Ag^+ , Cu^{2+} , Fe^{3+} , Hg^{2+} , Ca^{2+} , Mg^{2+} , Cd^{2+} , Pb^{2+} , Zn^{2+} individually in a dimethylformamide (DMF) solution, the fluorescence and absorbance spectra of 1×10^{-5} M SNDI, at excitation wavelengths of 225 nm and 360 nm were monitored to investigate the ion binding properties of SNDI in the polar aprotic solvent, DMF.

Chapter 4

DATA AND CALCULATIONS

4.1 Molar Calculations

In order to calculate the molar calculations of the stock SNDI solution and various metal cation solutions, dilution equation is used.

$$M_1V_1 = M_2V_2$$

Where;

M_1 : Initial concentration

V_1 : Initial volume

M_2 : Final concentration

V_2 : Final volume

20 microlitre of metal cations: 6.7×10^{-8} M

100 microlitre of metal cations: 3.33×10^{-7} M

150 microlitre of metal cations: 5×10^{-7} M

200 microlitre of metal cations: 6.67×10^{-7} M

300 microlitre of metal cations: 1×10^{-6} M

400 microlitre of metal cations: 1.33×10^{-6} M

500 microlitre of metal cations: 1.67×10^{-6} M

600 microlitre of metal cations: 2×10^{-6} M

700 microlitre of metal cations: 2.33×10^{-6} M

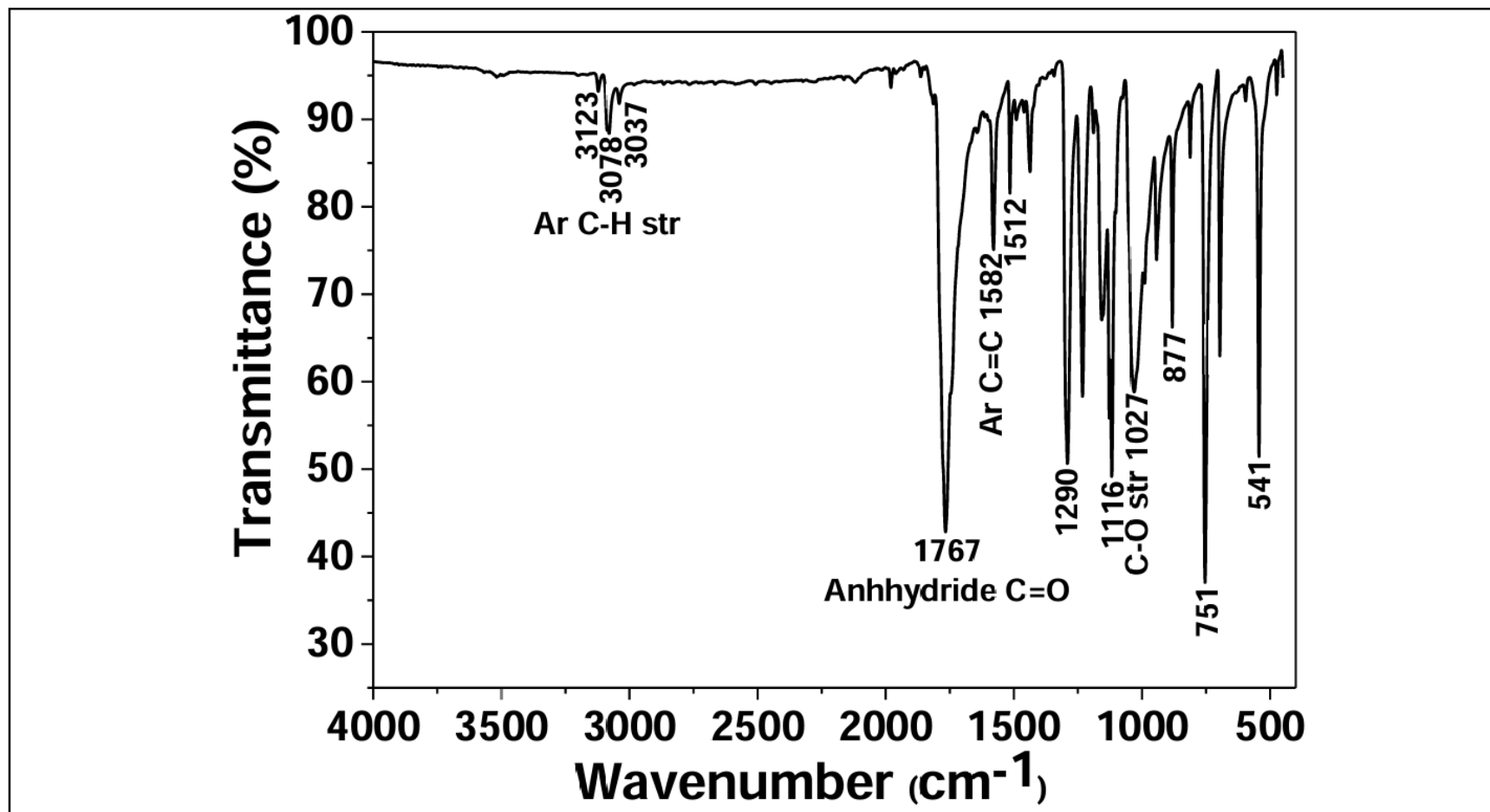


Figure 4.1: FT-IR spectrum of 1,4,5,8-Naphthalenetetracarboxylic dianhydride (NDA), KBr pellet.

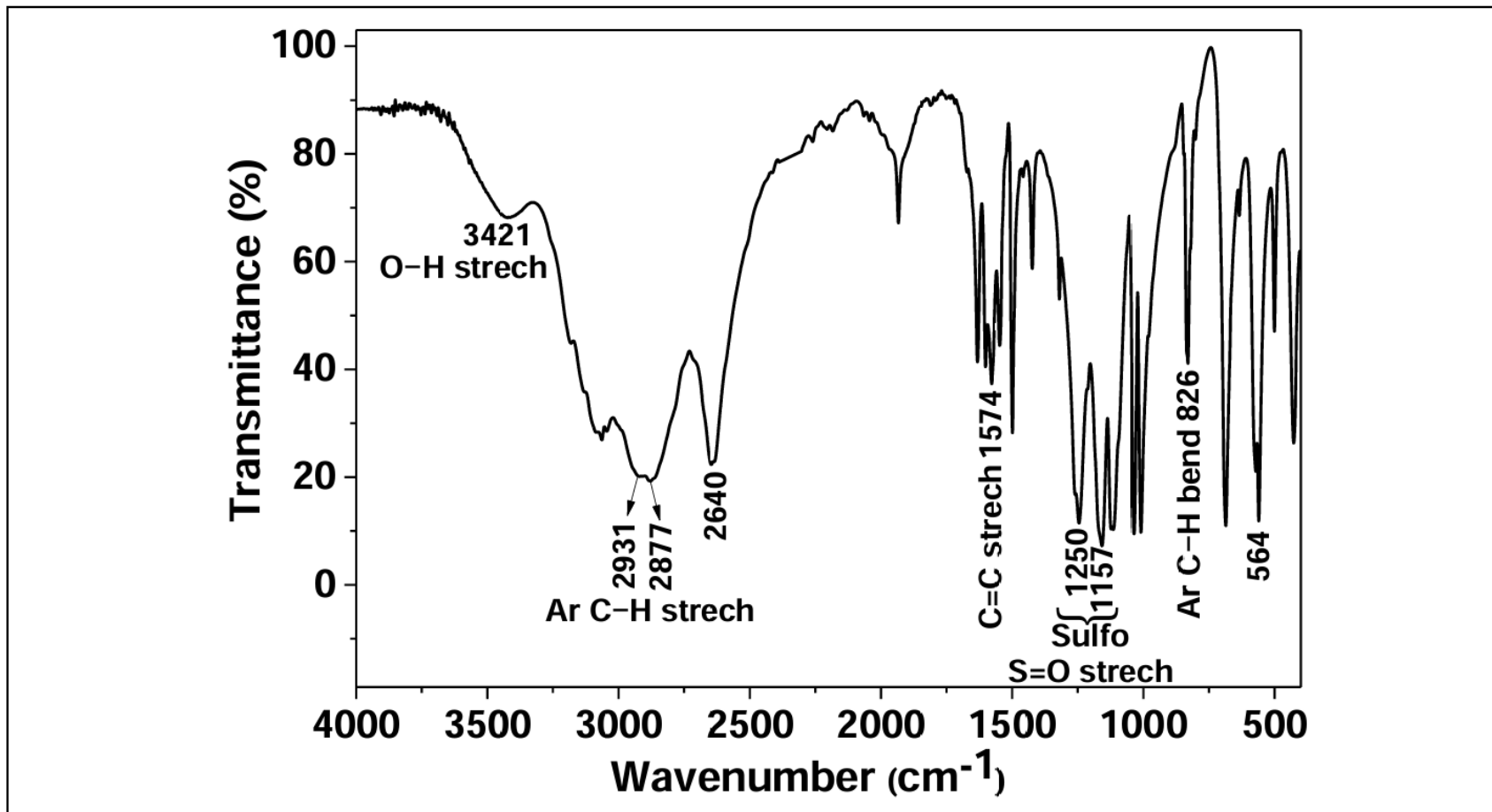


Figure 4.2: FT-IR spectrum of 4-aminobenzenesulfonic acid, KBr pellet.

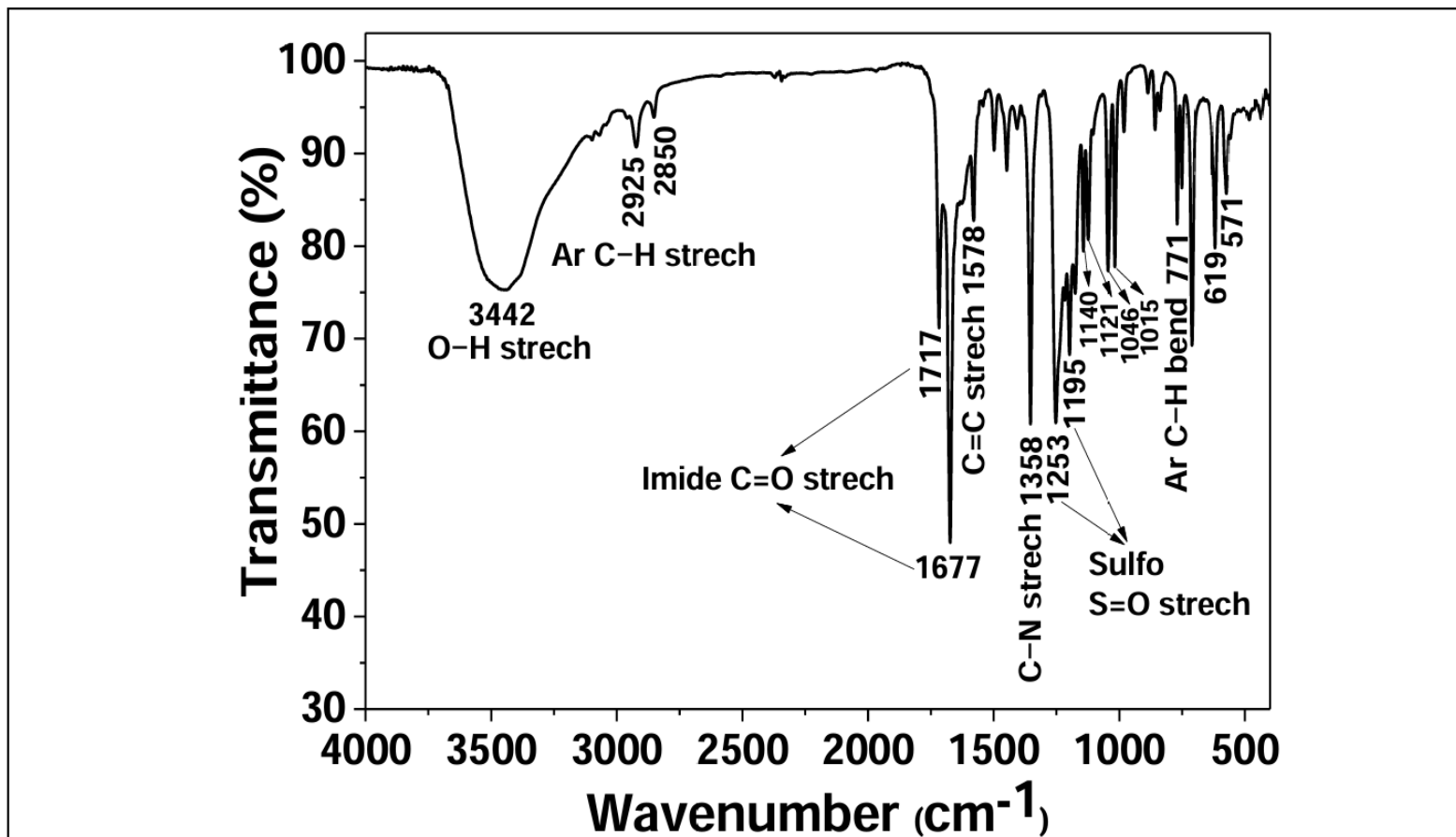


Figure 4.3: FT-IR spectrum of N, N'-bis(4-sulfohenyl)-1,4,5,8-naphthalene diimide (SNDI).

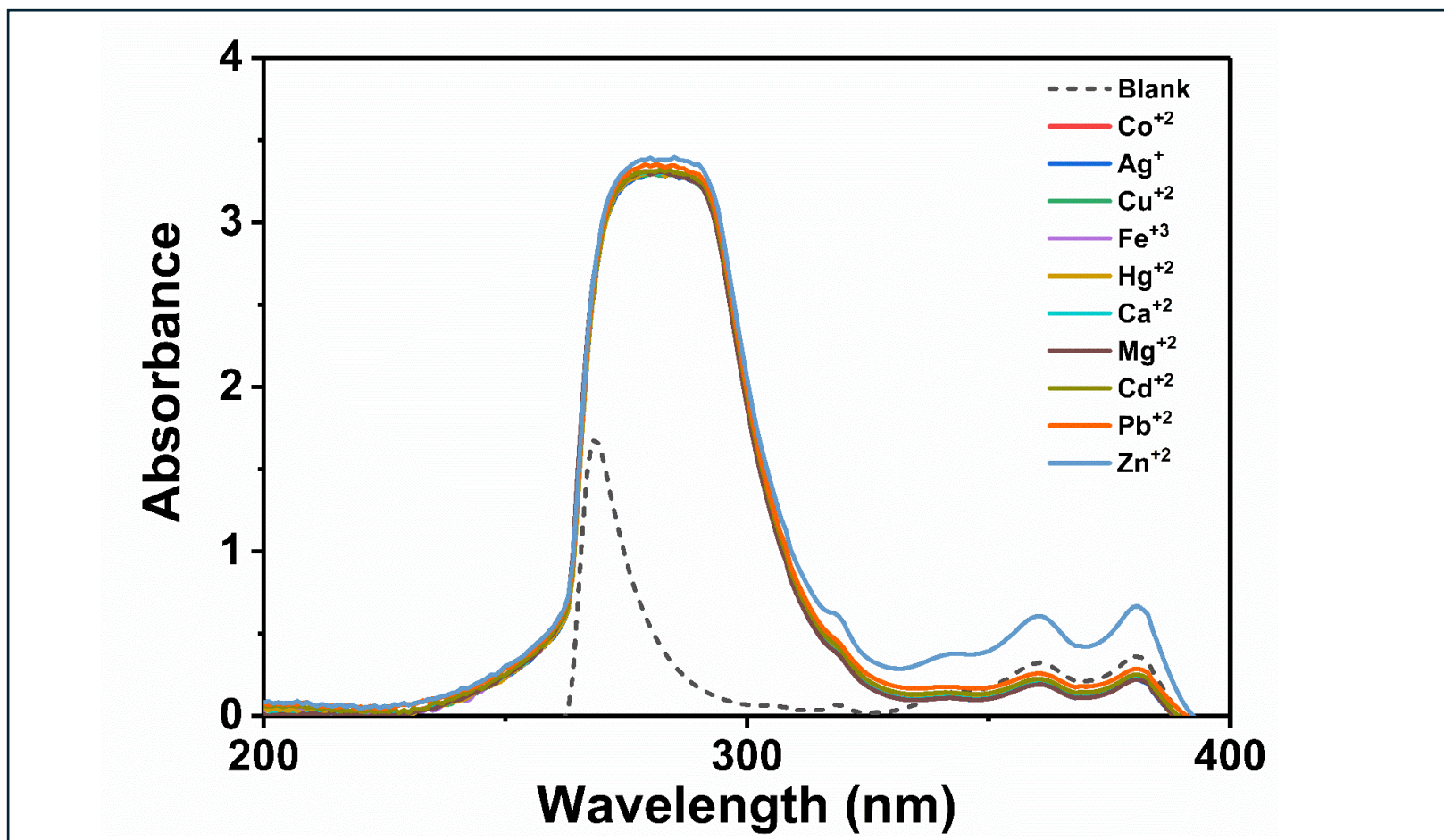


Figure 4.4: UV-vis absorption spectra of SNDI in the presence of metal ions.

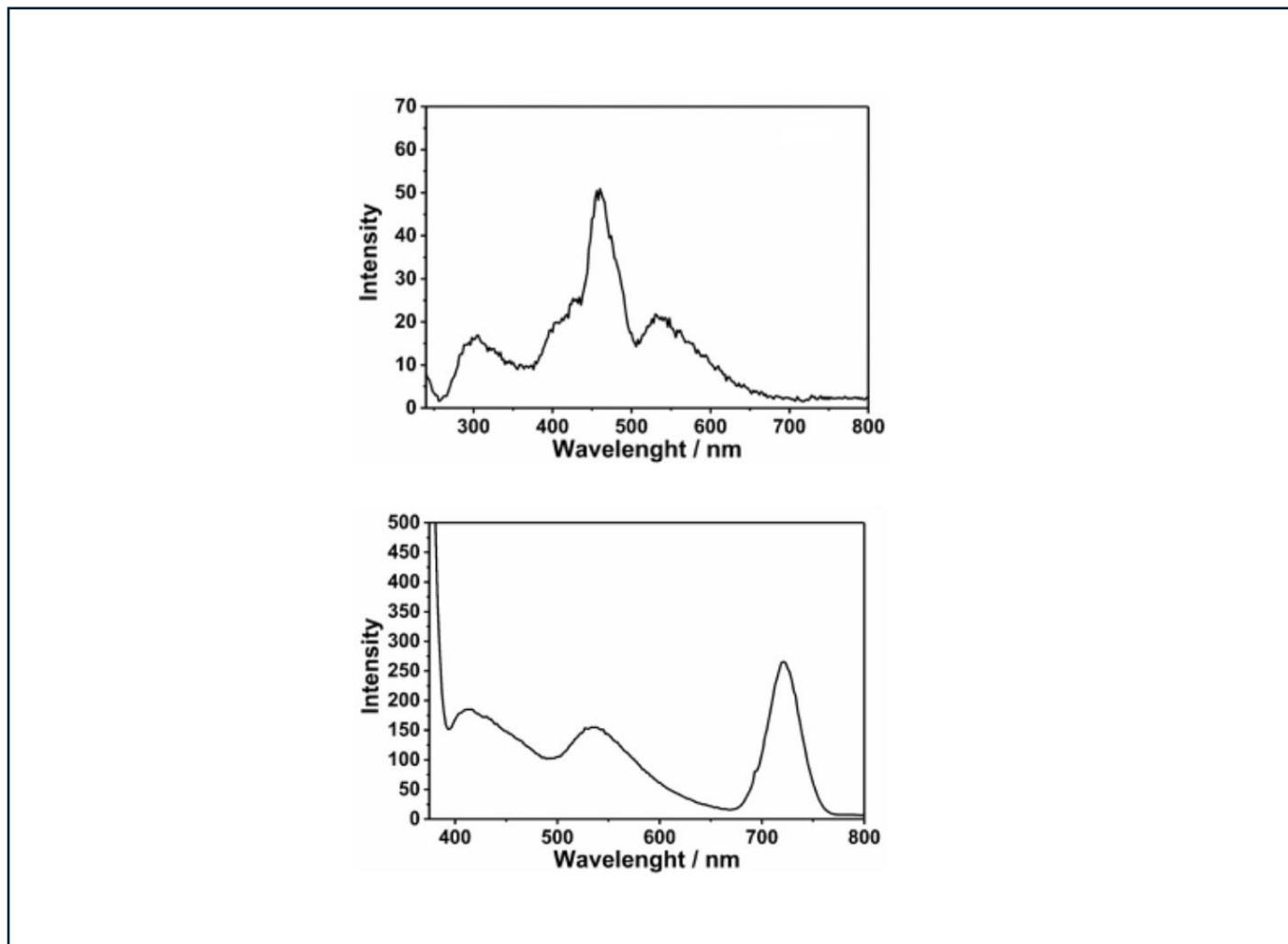


Figure 4.5: UV-vis emission spectra of SNDI in DMF at excitation wavelength of 225 nm (top) 360 nm (bottom).

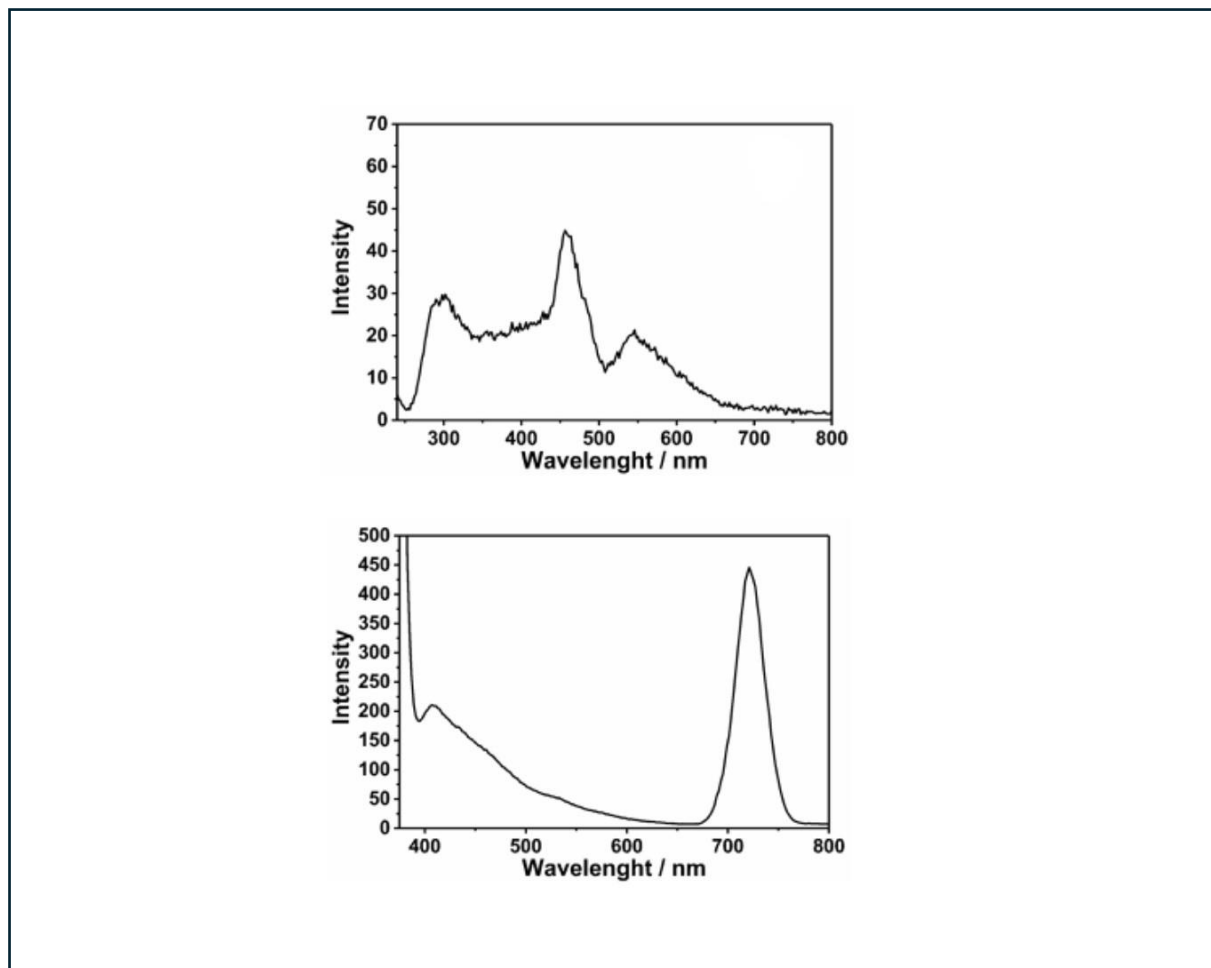


Figure 4.6: UV-vis emission spectra of 1.67×10^{-6} M Fe^{+3} in DMF at excitation wavelength of 225 nm (top) 360 nm (bottom).

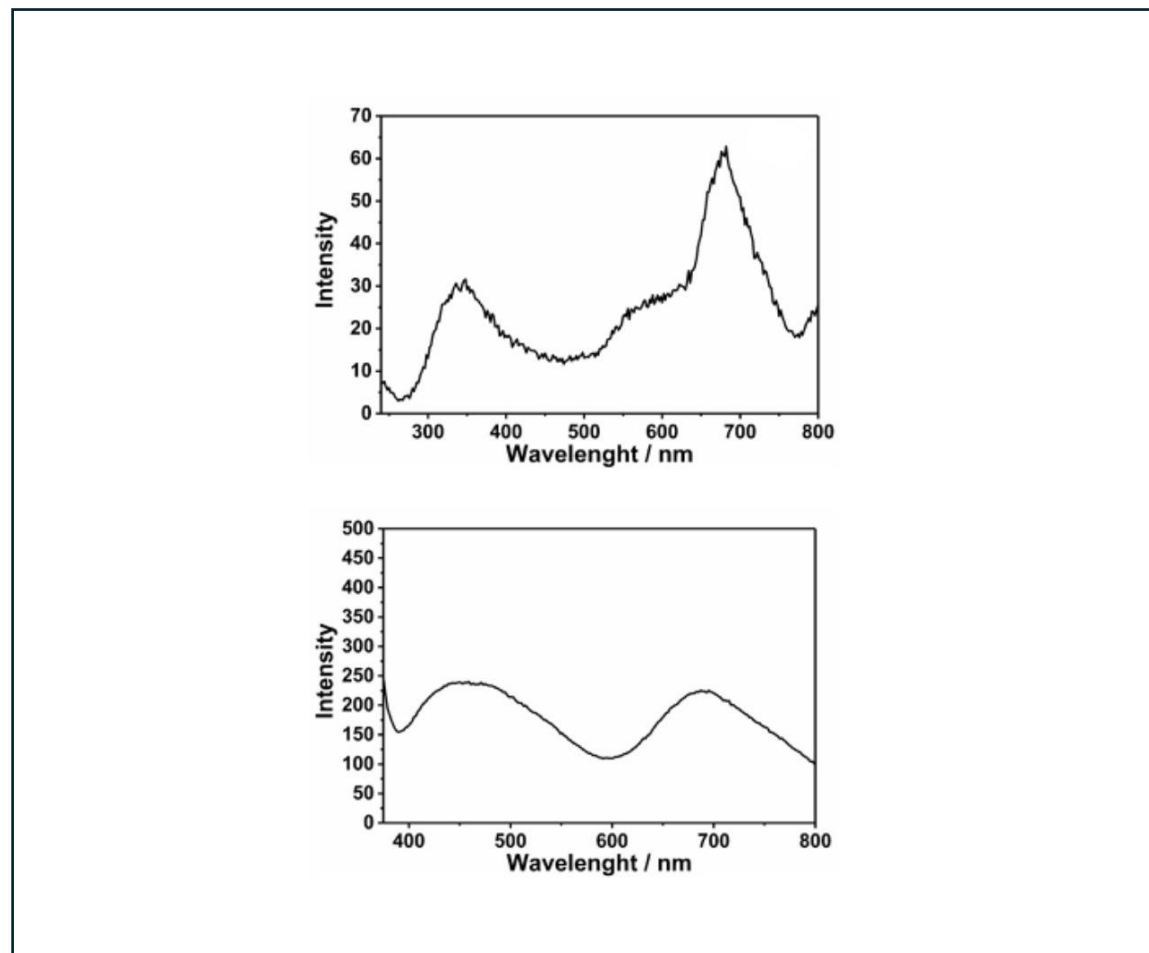


Figure 4.7: UV-vis emission spectra of SNDI with $1.67 \times 10^{-6} \text{ M Fe}^{3+}$ in DMF at excitation wavelength of 225 nm (top) 360 nm (bottom).

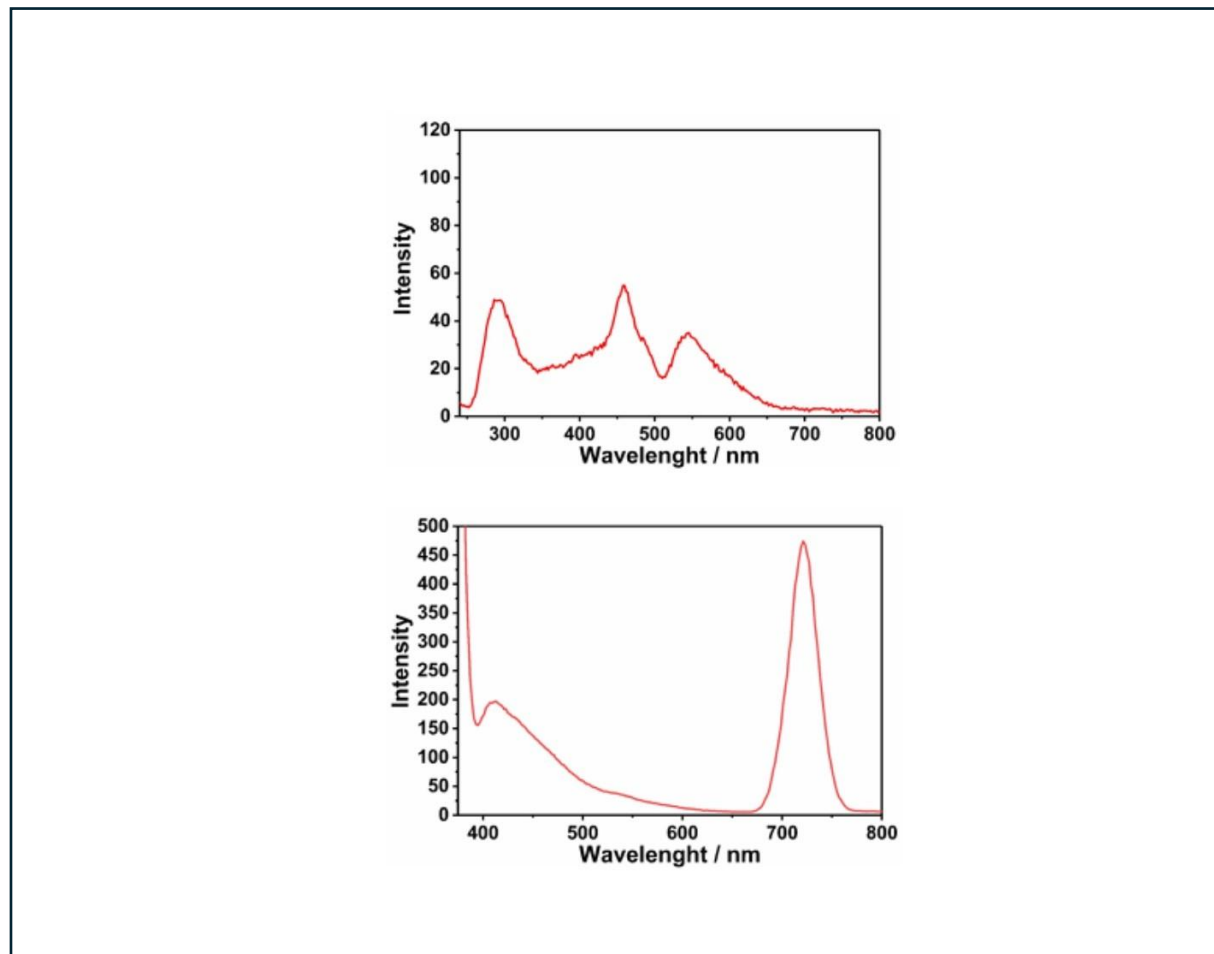


Figure 4.8: UV-vis emission spectra of 1.67×10^{-6} M Hg^{+2} in DMF at excitation wavelength of 225 nm (top) 360 nm (bottom).

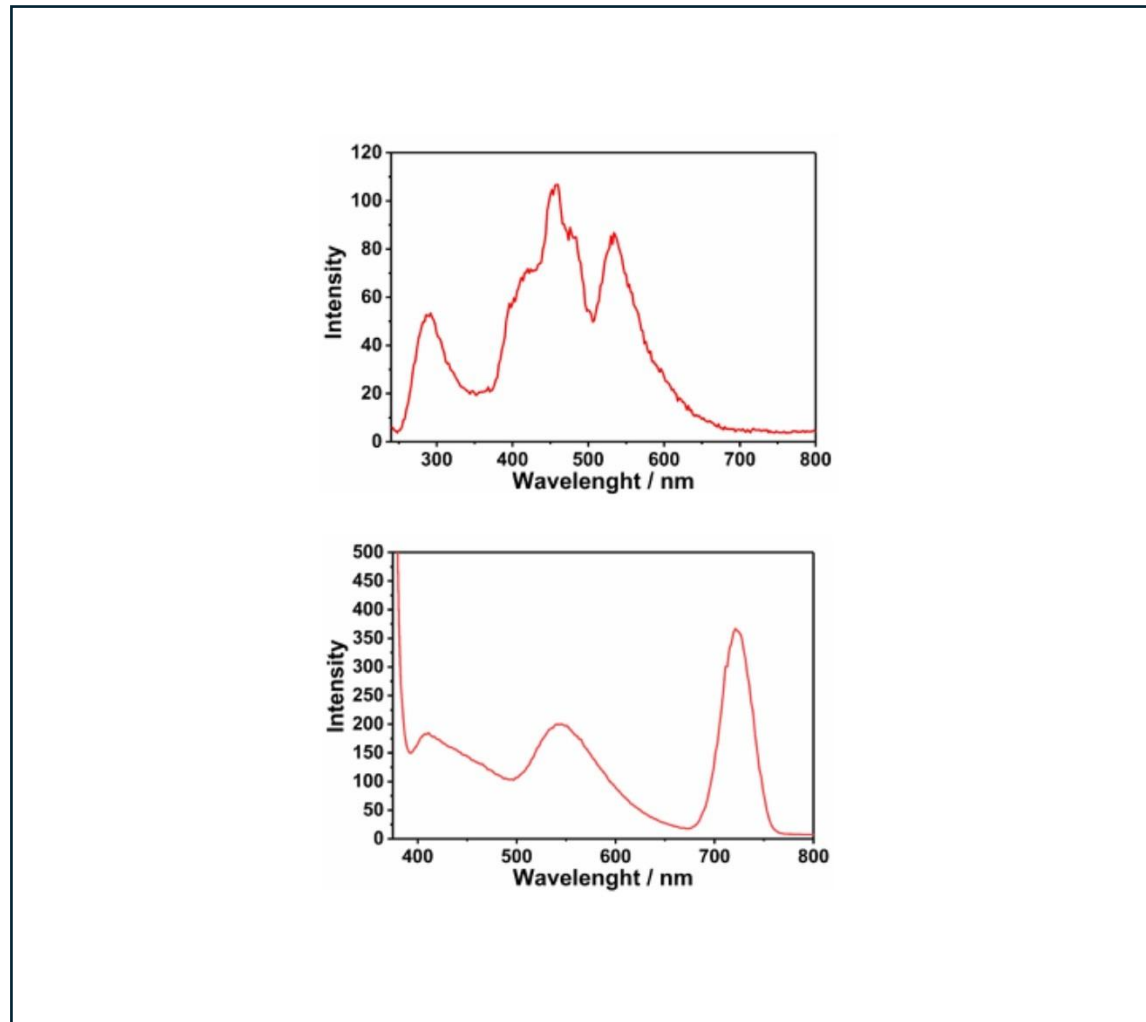


Figure 4.9: UV-vis emission spectra of $1.67 \times 10^{-6} \text{ M Hg}^{+2}$ in DMF at excitation wavelength of 225 nm (top) 360 nm (bottom).

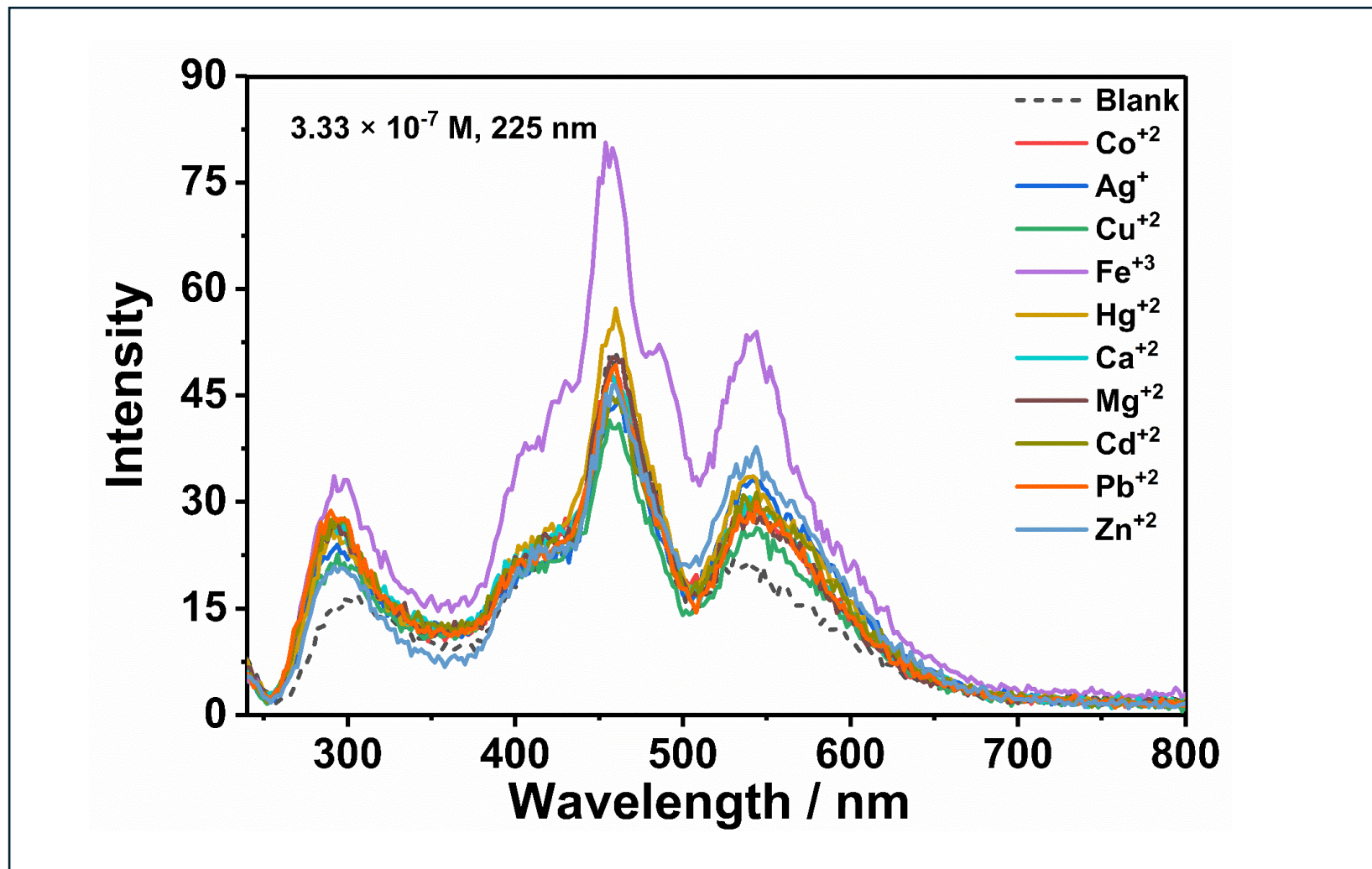


Figure 4.10: UV-vis emission spectra of SNDI in DMF in the presence of 3.33×10^{-7} M metal ions at excitation wavelength 225 nm.

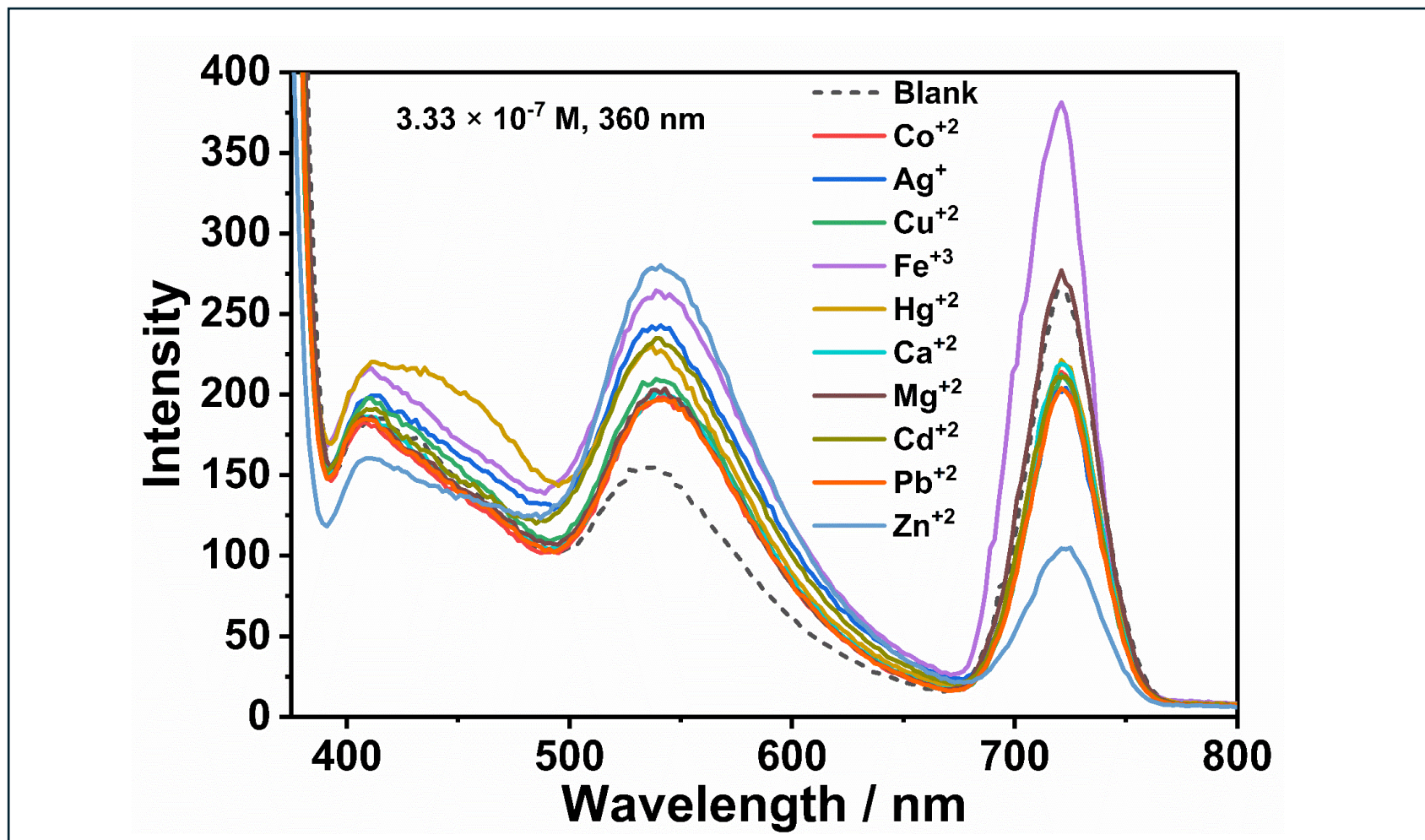


Figure 4.11: UV-vis emission spectra of SNDI in DMF in the presence of 3.33×10^{-7} M metal ions at excitation wavelength 360 nm.

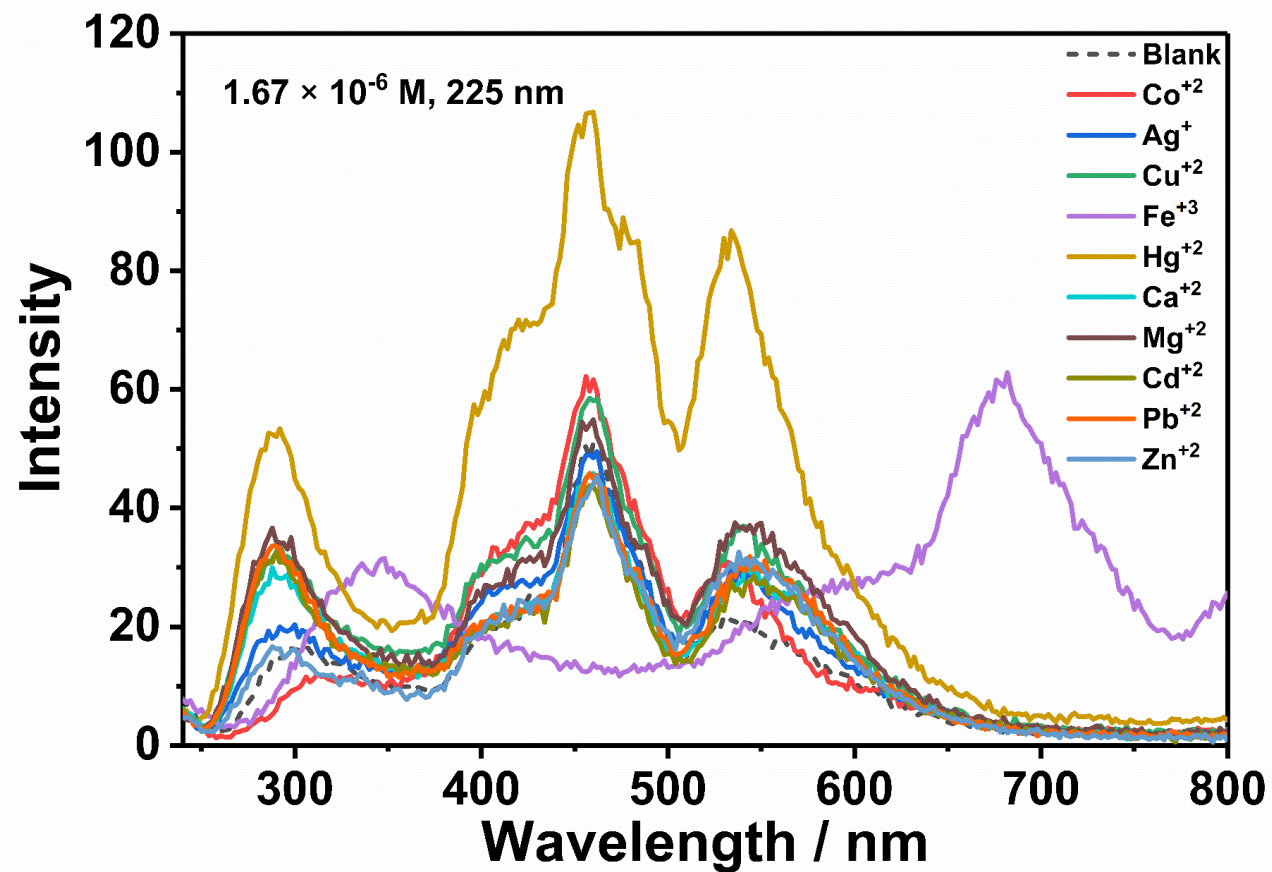


Figure 4.12: UV-vis emission spectra of SNDI in DMF in the presence of 1.67×10^{-6} M metal ions at excitation wavelength 225 nm.

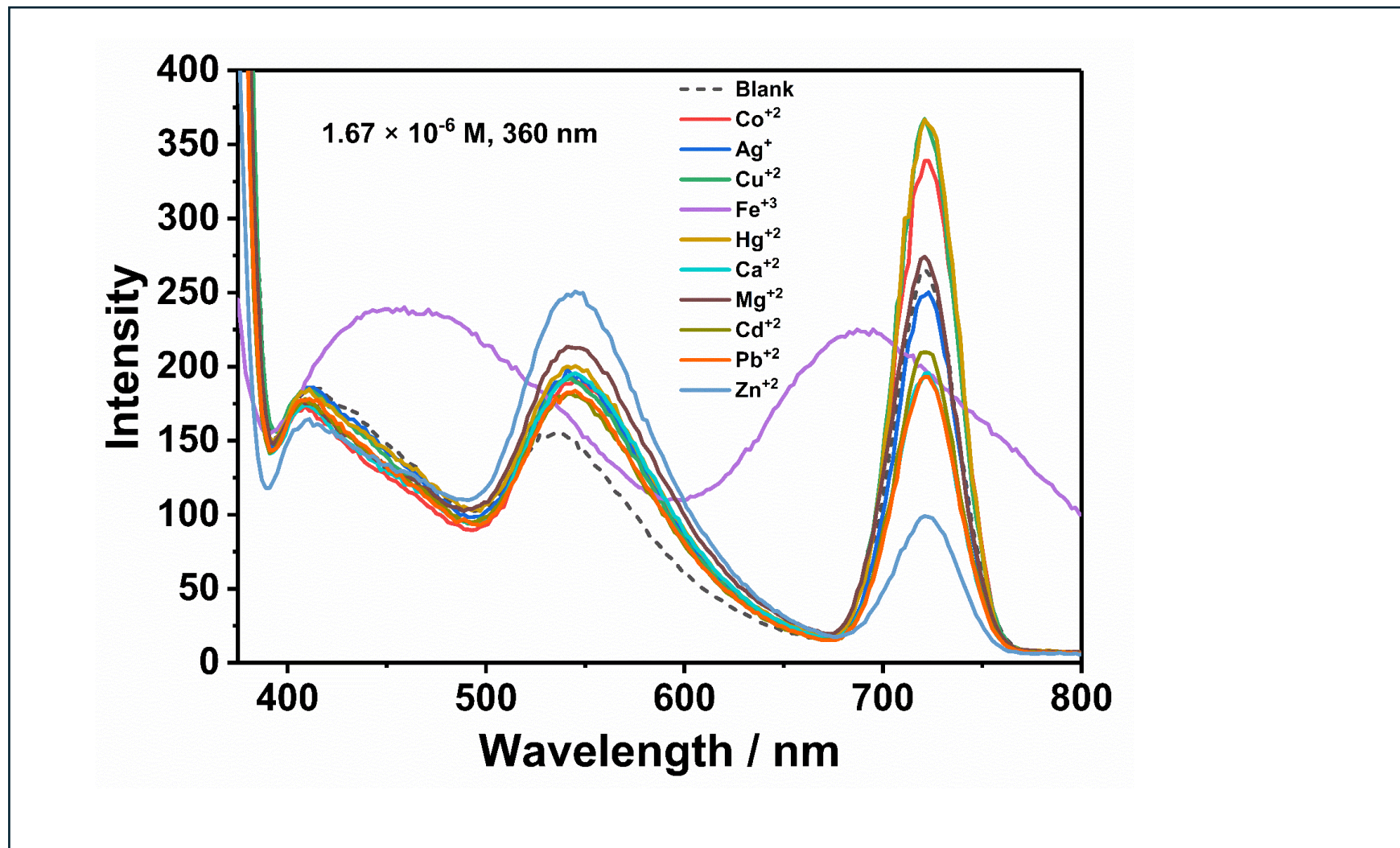


Figure 4.13: UV-vis emission spectra of SNDI in DMF in the presence of 1.67×10^{-6} M metal ions at excitation wavelength 360 nm.

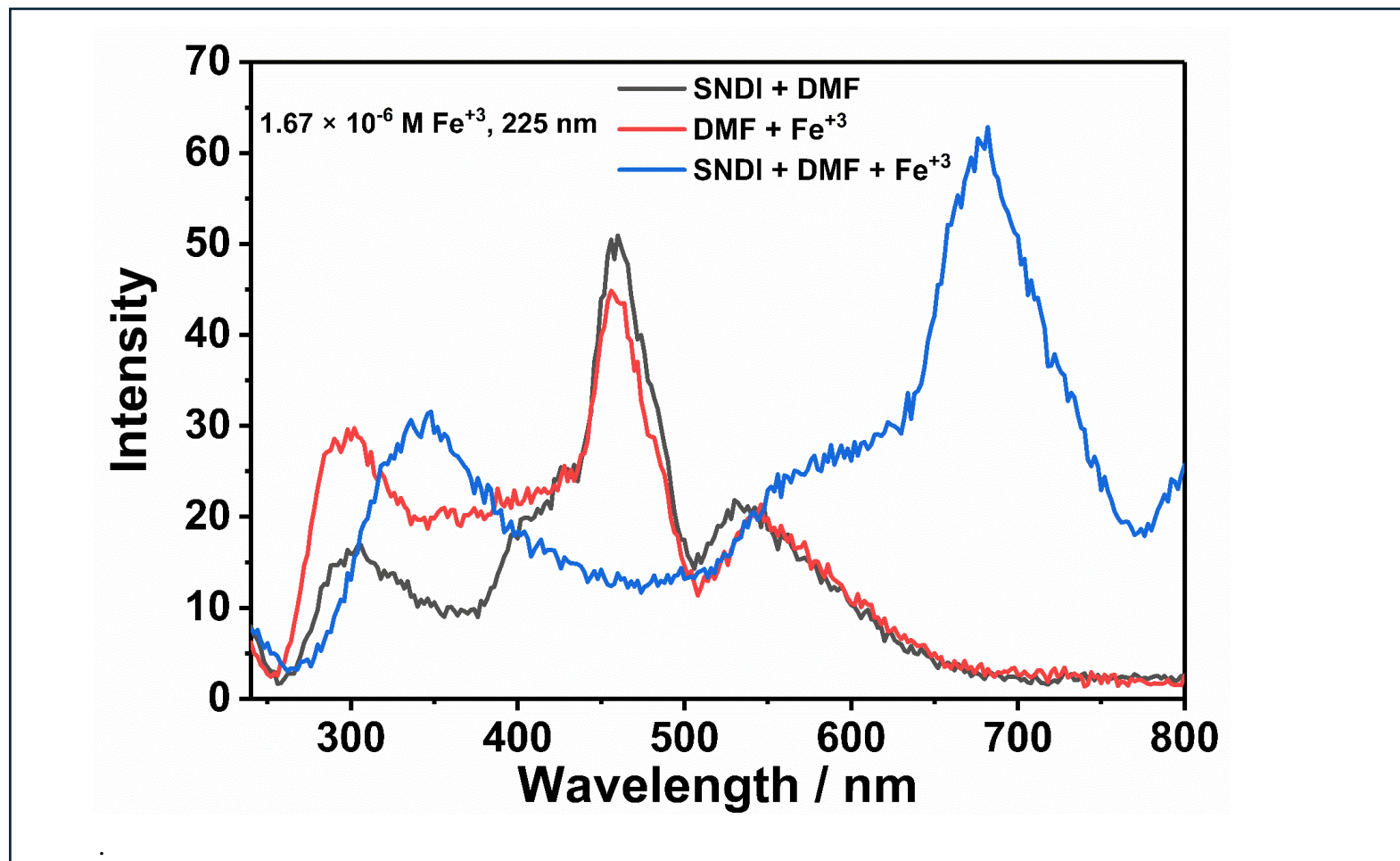


Figure 4.14: UV-vis emission spectra of SNDI in the presence of 1.67×10^{-6} M Fe^{+3} solution and DMF at excitation wavelength 225 nm.

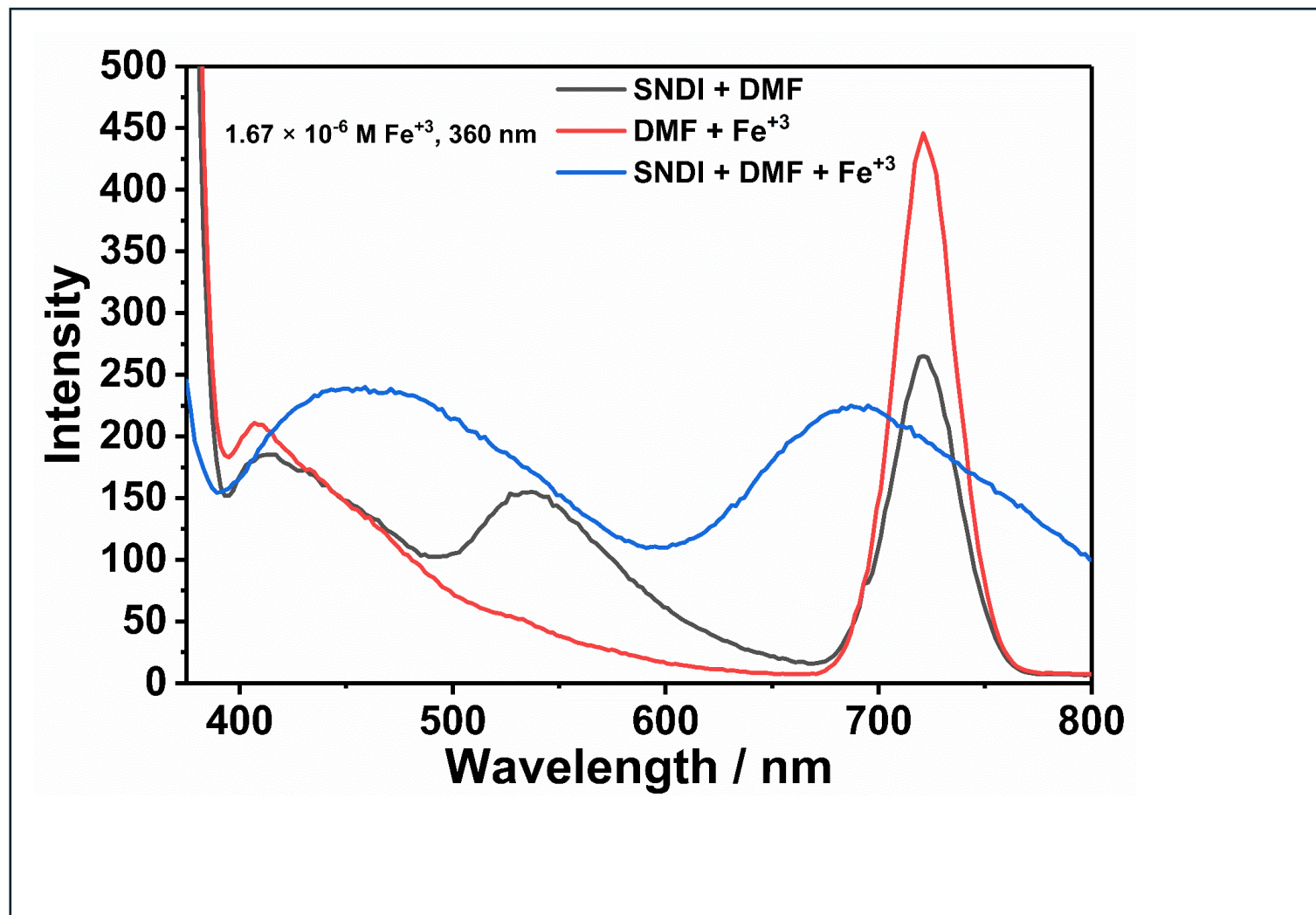


Figure 4.15: UV-vis emission spectra of SNDI in the presence of 1.67×10^{-6} M Fe^{+3} solution and DMF at excitation wavelength 360 nm.

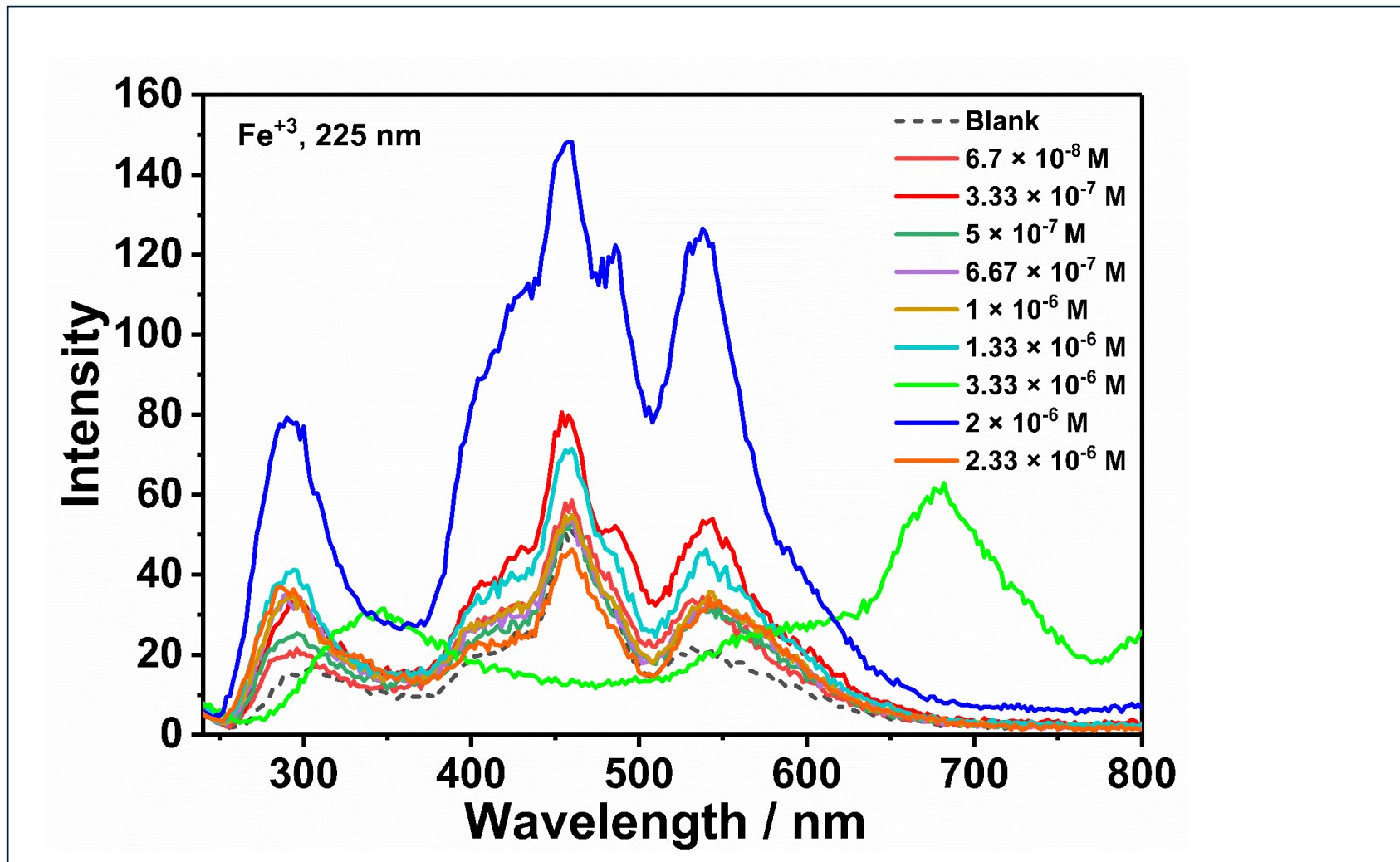


Figure 4.16: UV-vis emission spectra of SNDI in various concentrations of Fe³⁺ in DMF at excitation wavelength 225 nm.

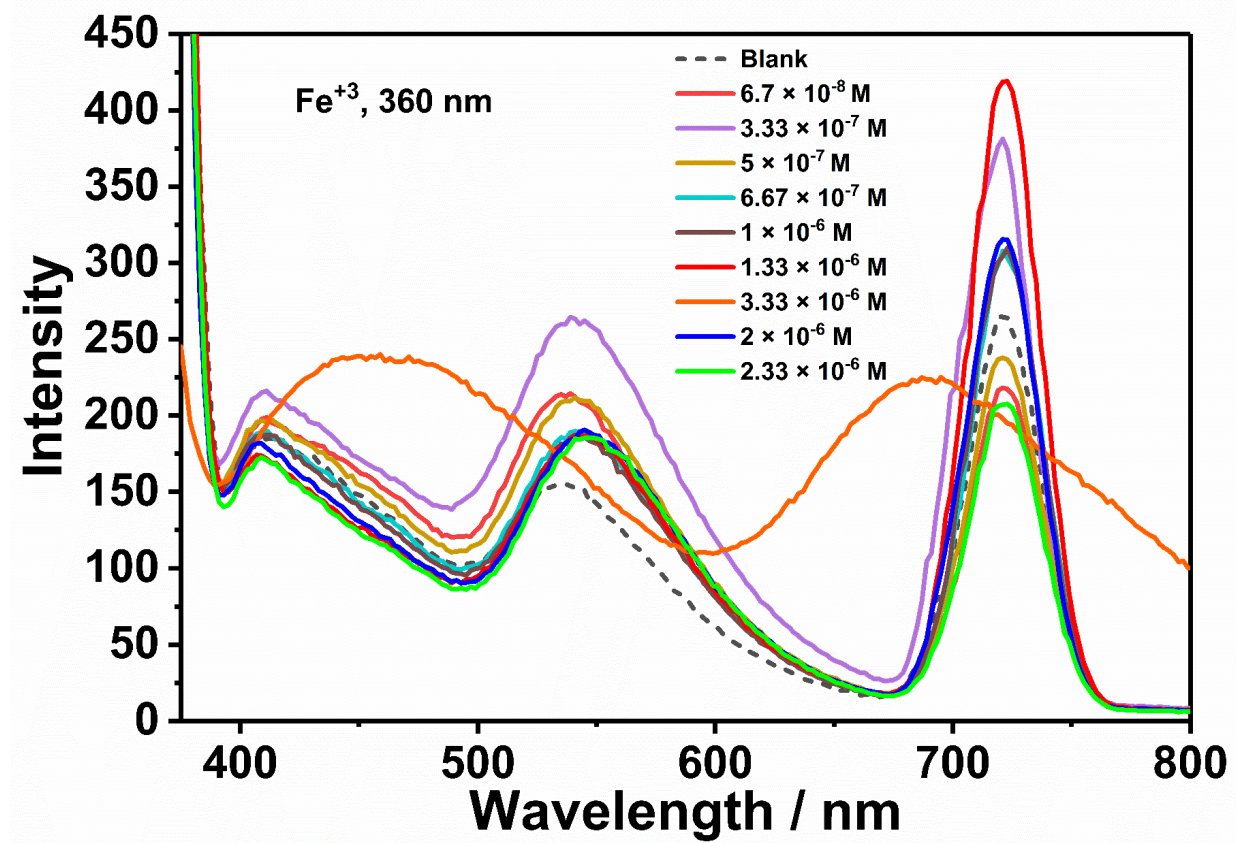


Figure 4.17: UV-vis emission spectra of SNDI in various concentrations of Fe³⁺ in DMF at excitation wavelength 360 nm.

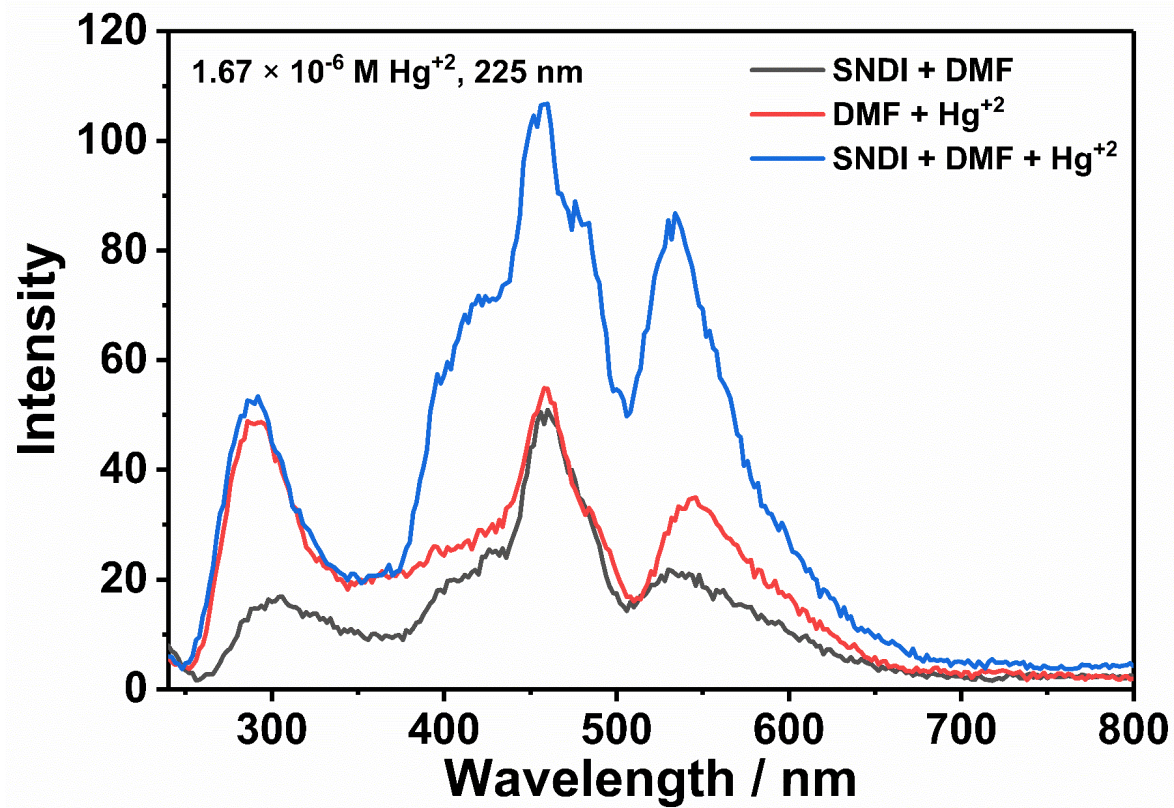


Figure 4.18: UV-vis emission spectra of SNDI in the presence of 1.67×10^{-6} M Hg⁺² solution and DMF at excitation wavelength 225 nm.

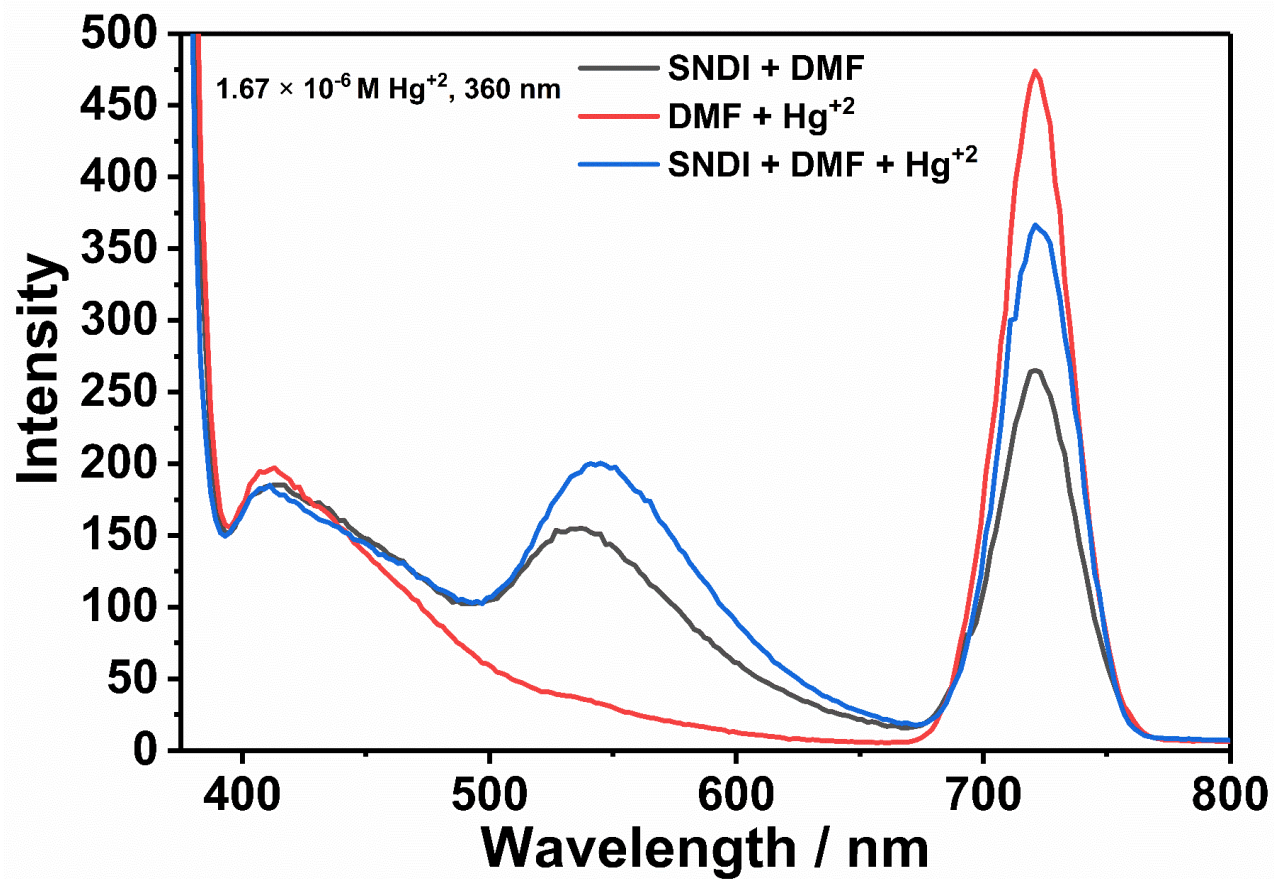


Figure 4.19: UV-vis emission spectra of SNDI in the presence of 1.67×10^{-6} M Hg^{+2} solution and DMF at excitation wavelength 360 nm.

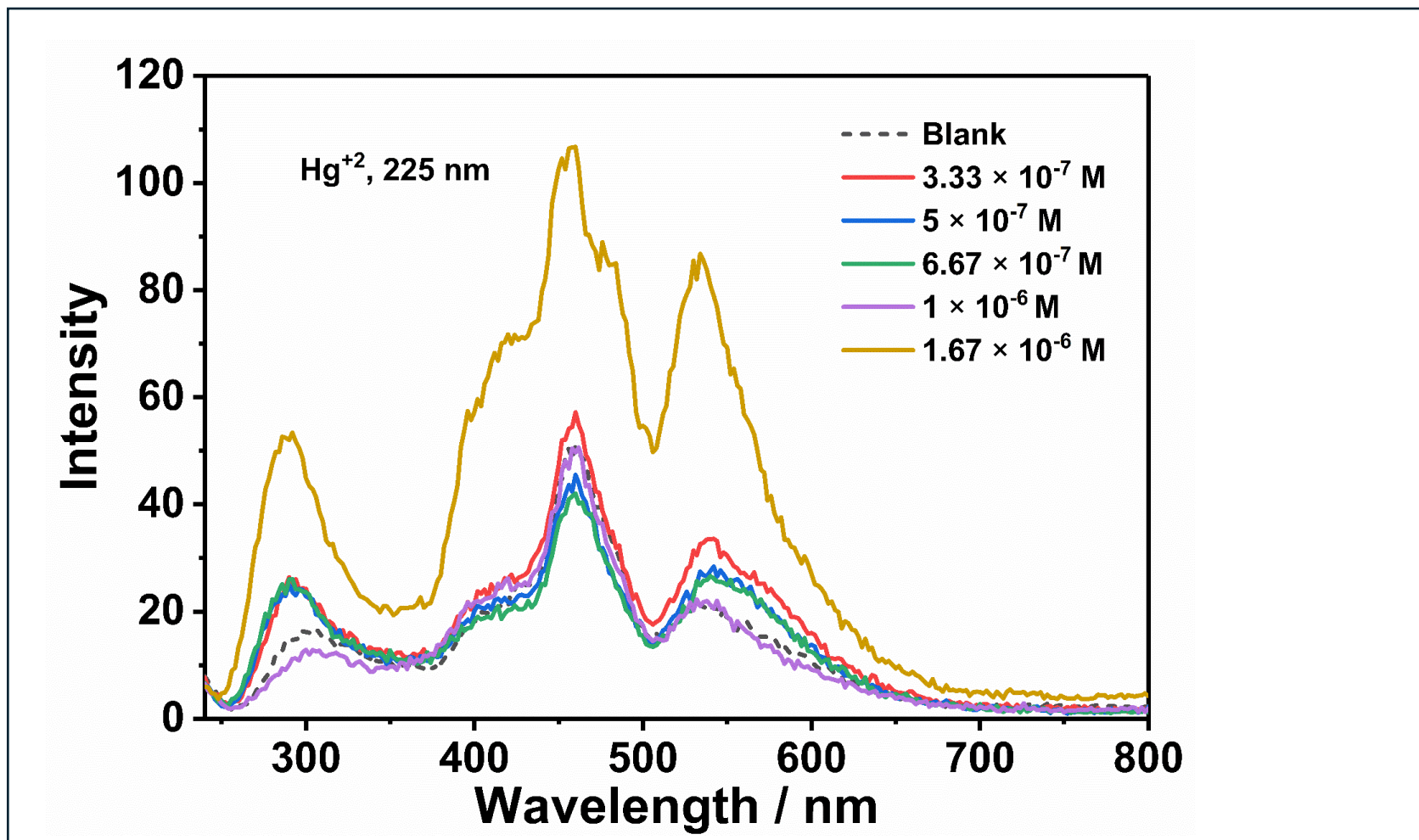


Figure 4.20: UV-vis emission spectra of SNDI in various concentrations of Hg^{+2} in DMF at excitation wavelength 225 nm.

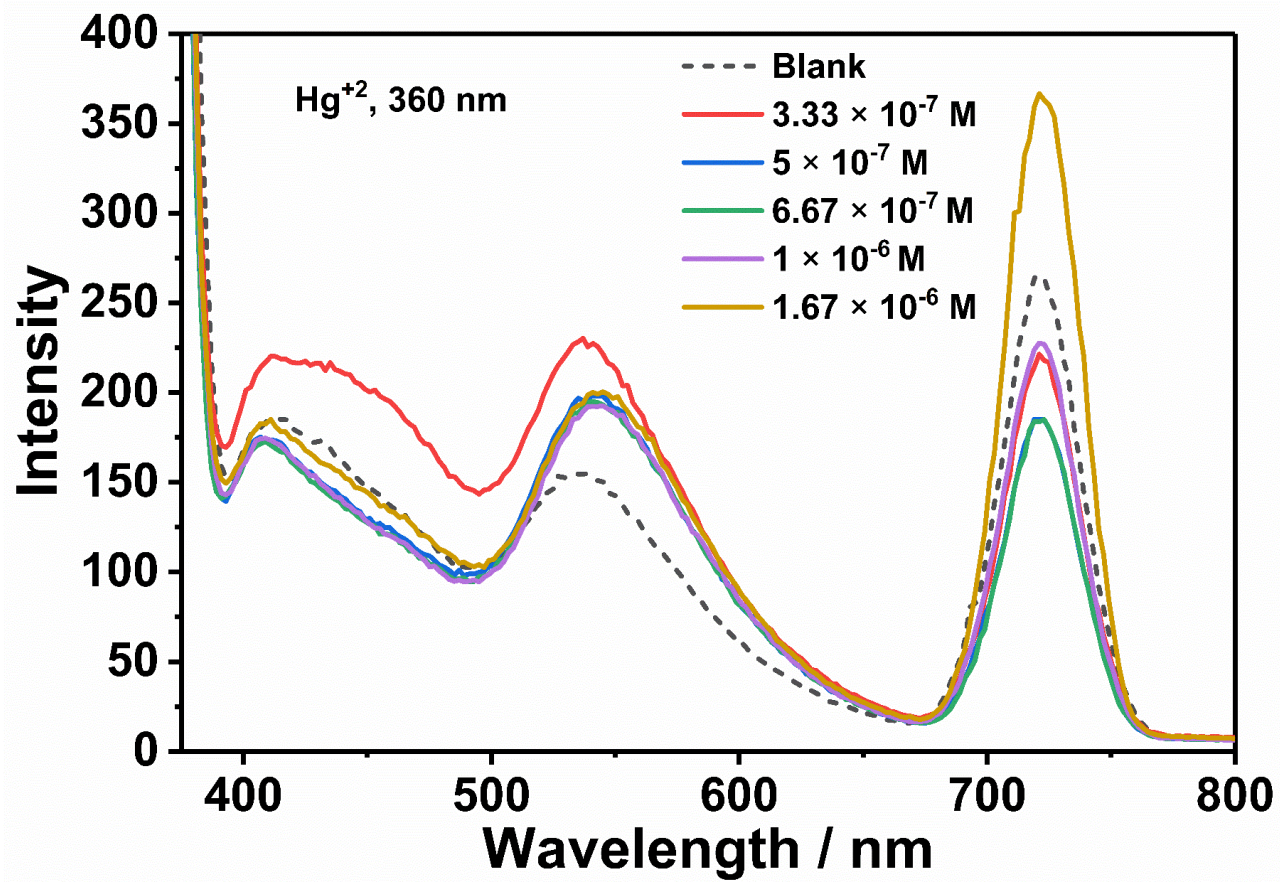


Figure 4.21: UV-vis emission spectra of SNDI in various concentrations of Hg^{2+} in DMF at excitation wavelength 360 nm.

Chapter 5

RESULTS AND DISCUSSION

5.1 Synthesis of SNDI

Through a condensation reaction, high percent yield of symmetric naphthalene diimide (SNDI) was synthesized in this research. This compound's synthesis route and mechanism of the reaction are shown in Figure 3.1 to Figure 3.5. The chemical structure of the produced compound was confirmed by FT-IR spectroscopy analysis.

5.2 FT-IR Spectra Analysis of SNDI

The IR spectrum of SNDI revealed that the typical peaks for anhydride carbonyl stretching, which were previously visible at 1767 cm^{-1} (as shown in Figure 4.3), had disappeared. New peaks replaced the former peaks in 1717 and 1677 cm^{-1} , corresponding to imide carbonyl stretching. Similarly, the distinct C-O-C stretching peak at 1027 cm^{-1} was no longer present and was substituted by a C-N stretch peak at 1358 cm^{-1} . Figure 4.2 shows the infrared spectra of aminobenzene sulfonic acid for reference.

5.3 Solubility of SNDI

SNDI demonstrates its pronounced solubility in polar aprotic solvents, specifically DMF and DMSO, as well as in polar protic solvents, including H_2O and HEPES, at room temperature. Additionally, SNDI exhibits partial solubility in other polar protic solvents, such as MeOH and EtOH, under the same conditions. Table 5.1 displays the solubility profile of SNDI of several solvents.

Table 5.1 : Solubility table of SNDI in several solvents.

Solvent	Solubility ^a / colour
	SNDI
THF	(- -)
ACE	(- -)
CHL	(- -)
PYR	(+ -) / yellow
EtOH	(+ -) / yellow
MeOH	(+ -) / yellow
CH ₃ CN	(+ -) / yellow
DMF	(+ +) / yellow
DMSO	(+ +) / yellow
H ₂ O	(+ +) / yellow
HEPES	(+ +) / yellow

^a: A concentration of 1M in solvents at room temperature.

(- -): insoluble.

(+ -): partially soluble at room temperature.

(+ +): soluble.

5.4 UV-Vis Absorption and Emission Spectra Analysis of SNDI

Figure 4.4 and Figure 4.5 respectively illustrate the absorption and emission spectra of SNDI at a concentration of 1.0×10^{-5} M the polar aprotic solvents DMF at room temperature. In Figure 4.5, the fluorescence spectra measured at an excitation wavelength of 225 nm, display broad excimer-like bands in DMF, covering a range of 300–600 nm. Similarly, spectra measured at excitation wavelength of 360 nm exhibit excimer-like bands extending from 400 to 800 nm.

5.5 UV-Vis Absorption and Emission Spectra Analysis of SNDI with Metal Cations

Figure 4.10 shows the emission spectrum of 1.0×10^{-5} M SNDI in DMF, with the presence of 3.33×10^{-7} M of metal cations, Co^{2+} , Ag^+ , Cu^{2+} , Fe^{3+} , Hg^{2+} , Ca^{2+} , Mg^{2+} , Cd^{2+} , Pb^{2+} , Zn^{2+} at the excitation wavelength of 225 nm. The blank used in all the spectra measurements is 1.0×10^{-5} M SNDI dissolved in DMF. It is apparent that addition of metal cations yields in an increase in intensity. Slight increase in all cations means that there is a mild sensing of the metals by the SNDI. However, addition of Fe^{3+} results in the most significant result out of all the cations, with all the peaks increasing significantly, (30 intensity at 300 nm, 80 intensity at 475 nm). This means that SNDI detects Fe^{3+} best at 3.33×10^{-7} M, showing a fluorescence on sensor property to Fe^{3+} . Figure 4.11 shows the emission spectrum of 1.0×10^{-5} M SNDI in DMF, with the presence of 3.33×10^{-7} M of metal cations at the excitation wavelength of 360 nm. This spectrum confirms the Fe^{3+} sensing of the SNDI, with the Fe^{3+} peak being the highest around 400 intensity comparably higher than the other cation peaks. This result can be explained due to Fe^{3+} cation forming a complex with the carbonyl group of the naphthalene core of SNDI.

Figure 4.12 depicts the emission spectrum of 1.0×10^{-5} M SNDI in DMF with the presence of 1.67×10^{-6} M of metal cations at the excitation wavelength of 225 nm. At higher concentrations, addition of Hg^{2+} and Fe^{3+} cations shows a remarkable result. Hg^{2+} peak increases in intensity, meaning that SNDI acquires fluorescence on sensor properties at this concentration. On the other hand, Fe^{3+} peak at this concentration seems to be red shifting, due to the peak present around 700 nm. Figure 4.13 shows the emission spectrum of same conditions, but with an excitation wavelength of 360

nm. With Hg^{+2} peak being the most intense, and Fe^{+3} peak being shifted compared to other cation peaks, this spectrum confirms the results obtained from the spectrum of 225 nm excitation wavelength.

Figure 4.14 shows the comparison of the emission spectrum of the SNDI, Fe^{+3} cations and their complexation respectively at excitation wavelength of 225 nm. 1.0×10^{-5} M SNDI in DMF and 1.67×10^{-6} M Fe^{+3} in DMF show a similar result, with peaks having similar intensities at similar wavelengths. However, when Fe^{+3} solution is added to the SNDI, it becomes apparent that there is an increase in intensity, as well as the shifting of the peaks towards the IR region. Figure 4.15 confirms this shift at excitation wavelength of 360 nm.

Figure 4.16 shows 1.0×10^{-5} M SNDI in DMF with various concentrations of Fe^{+3} cations at excitation wavelength of 225 nm. It can be deduced that fluorescence on property of SNDI to Fe^{3+} cations are present from 6.7×10^{-8} M to 2×10^{-6} M, which then starts to quench at 2.33×10^{-6} M. A special shifting property is observed at 1.67×10^{-6} M, which is partially observed with 2.33×10^{-6} M as well. This can be due to a complexation with the sulfonyl group in SNDI, which causes the red shifted excimer emission. In Figure 4.17, we look at the same spectrum with excitation wavelength of 360 nm. It is observed that maximum fluorescence enhancement is at 6.7×10^{-8} M. Fluorescence on property of SNDI is up to 3.33×10^{-7} M on the 0-1 band. The complexation which occurs at 1.67×10^{-6} M that causes the red shifted enhanced emission is also present in this spectrum.

Figure 4.18 shows the comparison of the emission spectrum of SNDI, Hg^{+2} cations and their complexations, respectively. At excitation wavelength of 225 nm. 1.0×10^{-5}

M SNDI in DMF and 1.67×10^{-6} M Hg^{+2} in DMF show a similar result, with peaks having similar intensities at similar wavelengths. However, when Hg^{+2} solution is added to the SNDI, it becomes apparent that there is a significant increase in the intensity. The notion of fluorescence on sensor property of SNDI to Hg^{+2} cations can be deduced with an excimer type emission, due to a complexation through the sulfonyl part of SNDI. Figure 4.19 shows the same spectrum at excitation wavelength of 360 nm. It can be observed that the fluorescence on property dissipates at this excitation wavelength. Due to the intensity of SNDI with Hg^{+2} cations in DMF decreasing in intensity.

Figure 4.20 illustrates SNDI in various concentrations of Hg^{+2} cations in DMF, at excitation wavelength of 225 nm. Fluorescence on property of SNDI to Hg^{+2} is present up to 1.67×10^{-6} M Hg with an excimer type emission can be observed due to a complexation of Hg^{+2} cations with sulfonyl group of SNDI. This fluorescence on property is also present in the spectrum displayed in Figure 4.21, in which the excitation wavelength is 360 nm. Same deduction can be made about the complexation of Hg^{+2} through naphthalene carbonyls in this spectrum.

Chapter 6

CONCLUSION

In this study, a derivative of naphthalene diimide, previously reported in the literature, N,N'-bis(4-sulfophenyl)-1,4,5,8-naphthalene diimide (SNDI), was resynthesized, characterised, and evaluated for its selectivity as a chemosensor for several metal cations. The sensitivity of SNDI toward a range of metal ions, including Co^{2+} , Ag^+ , Cu^{2+} , Fe^{3+} , Hg^{2+} , Ca^{2+} , Mg^{2+} , Cd^{2+} , Pb^{2+} and Zn^{2+} were systematically investigated using UV-visible and fluorescence spectroscopy techniques. FT-IR spectroscopy measurements was utilised to confirm the chemical structure of the synthesized product.

SNDI, which incorporates metal-binding sites, demonstrated its ability to function as a selective and sensitive fluorescence chemosensor for the detection of Fe^{3+} and Hg^{2+} ions in a polar aprotic solution. The interaction between SNDI and Fe^{3+} , and of Hg^{2+} and was thoroughly examined using UV-visible spectroscopy, fluorescence spectroscopy.

In future studies, SNDI will be further explored as an electrochemical sensor, with a focus on evaluating its potential applicability as a functional chemosensor device, especially in another polar aprotic solvent, DMSO. Additionally, further derivatives of SNDI by core-substitution will be synthesized and examined for their chemosensor applications.

REFERENCES

- [1] Andreea Diac, Mihaela Matache, Ion Grosu and Hädade, N.D. (2018). Naphthalenediimide - A Unique Motif in Macrocyclic and Interlocked Supramolecular Structures. *360(5)*, 817–845.
- [2] Mohammad Al Kobaisi, Bhosale, S.V., Latham, K., Raynor, A.M. and Bhosale, S.V. (2016). Functional Naphthalene Diimides: Synthesis, Properties, and Applications. *116(19)*, 11685–11796.
- [3] Suraru, S.-L. and Würthner, F. (2014). Strategies for the Synthesis of Functional Naphthalene Diimides. *Angewandte Chemie International Edition*, *53(29)*, 7428–7448.
- [4] Bhosale, S.V., Jani, C.H. and Langford, S.J. (2008). Chemistry of naphthalene diimides. *Chem. Soc. Rev.*, *37(2)*, 331–342.
- [5] Ling, Q.-H., Zhu, J.-L., Qin, Y. and Xu, L. (2020). Naphthalene diimide- and perylene diimide-based supramolecular cages. *Materials Chemistry Frontiers*, *4(11)*, 3176–3189.
- [6] Peng, X., Wang, L. and Chen, S. (2021). Donor–acceptor charge transfer assemblies based on naphthalene diimides (NDIs). *Journal of Inclusion Phenomena and Macrocyclic Chemistry*, *99(3-4)*, 131–154.

- [7] Avinash, M.B. and Govindaraju, T. (2018). Architectonics: Design of Molecular Architecture for Functional Applications. *Accounts of Chemical Research*, 51(2), 414–426.
- [8] Vicic, D.A., Odom, D.T., Núñez, M.E., Gianolio, D.A., McLaughlin, L.W. and Barton, J.K. (2000). Oxidative Repair of a Thymine Dimer in DNA from a Distance by a Covalently Linked Organic Intercalator. *Journal of the American Chemical Society*, 122(36), 8603–8611.
- [9] Pengo, P., Pantoş, G.D., Otto, S. and Sanders, J.K.M. (2006). Efficient and Mild Microwave-Assisted Stepwise Functionalization of Naphthalenediimide with α -Amino Acids. *The Journal of Organic Chemistry*, 71(18), 7063–7066.
- [10] Pan, M., Lin, X.-M., Li, G.-B. and Su, C.-Y. (2011). Progress in the study of metal–organic materials applying naphthalene diimide (NDI) ligands. *Coordination Chemistry Reviews*, 255(15-16), 1921–1936.
- [11] Takenaka, S. (2021). Application of naphthalene diimide in biotechnology. *Polymer Journal*, [online] 53(3), 415–427.
- [12] Fukutomi, Y., Nakano, M., Hu, J.-Y., Osaka, I. and Takimiya, K. (2013). Naphthodithiophenediimide (NDTI): Synthesis, Structure, and Applications. *Journal of the American Chemical Society*, 135(31).

- [13] Reiß, B. and Wagenknecht, H.-A. (2019). Naphthalene diimides with improved solubility for visible light photoredox catalysis. *Beilstein Journal of Organic Chemistry*, 15, 2043–2051.
- [14] Röger, C. and Würthner, F. (2007). Core-Tetrasubstituted Naphthalene Diimides: Synthesis, Optical Properties, and Redox Characteristics. *The Journal of Organic Chemistry*, 72(21), 8070–8075.
- [15] Li, C., Lin, Z., Li, Y. and Wang, Z. (2016). Synthesis and Applications of π -Extended Naphthalene Diimides. *The Chemical Record*, 16(2), 873–885.
- [16] Sommer, M. (2014). Conjugated polymers based on naphthalene diimide for organic electronics. *J. Mater. Chem. C*, 2(17), 3088–3098.
- [17] Cox, R.P., Higginbotham, H.F., Graystone, B.A., Sandanayake, S., Langford, S.J. and Bell, T.D.M. (2011). A new fluorescent H⁺ sensor based on core-substituted naphthalene diimide. *Chemical Physics Letters*, [online] 521, 59–63.
- [18] Doria, F., Folini, M., Grande, V., Graziella Cimino-Reale, Zaffaroni, N. and Freccero, M. (2014). Naphthalene diimides as red fluorescent pH sensors for functional cell imaging. *Organic & Biomolecular Chemistry*, 13(2), 570–576.
- [19] Arwa Abourajab, Pelin Karsili, Rashid, R., Meltem Dinleyici, Nur Pasaogullari, Sinem Altınışık, Sermet Koyuncu and Huriye Icil (2024). A new water-soluble naphthalene diimide as a highly selective fluorescent chemosensor for Cu(II)

ion: Synthesis, DFT calculations, photophysical and electrochemical properties. *Journal of Photochemistry and Photobiology A Chemistry*, 454, 115719–115719.

- [20] Pandey, R., Kumar, A., Xu, Q. and Pandey, D.S. (2020). Zinc(II), copper(II) and cadmium(II) complexes as fluorescent chemosensors for cations. *Dalton Transactions*, 49(3), 542–568.
- [21] Pooja, Pandey, H., Aggarwal, S., Vats, M., Rawat, V. and Pathak, S.R. (2022). Coumarin-based Chemosensors for Metal Ions Detection. *Asian Journal of Organic Chemistry*, 11(12).
- [22] Anslyn, E.V.; Wang, B. (2011). Preface. In *Chemosensors Principles, Strategies, and Applications*; Wang, B., Anslyn, E.V., Eds.; John Wiley & Sons, *Wiley eBooks*, xi.
- [23] Petrucci, R., Pasquali, M., Scaramuzzo, F.A. and Curulli, A. (2021). Recent Advances in Electrochemical Chitosan-Based Chemosensors and Biosensors: Applications in Food Safety. *Chemosensors*, 9(9), 254.
- [24] Muhammad, M., Khan, S., Shehzadi, S.A., Gul, Z., Al-Saidi, H.M., Waheed Kamran, A. and Alhumaydhi, F.A. (2022). Recent advances in colorimetric and fluorescent chemosensors based on thiourea derivatives for metallic cations: A review. *Dyes and Pigments*, 205, 110477.

- [25] Gao, N., Yu, J., Tian, Q., Shi, J., Zhang, M., Chen, S. and Zang, L. (2021). Application of PEDOT:PSS and Its Composites in Electrochemical and Electronic Chemosensors. *Chemosensors*, 9(4), 79.
- [26] Krämer, J., Kang, R., Grimm, L.A., Luisa De Cola, Picchetti, P. and Biedermann, F. (2022). Molecular Probes, Chemosensors, and Nanosensors for Optical Detection of Biorelevant Molecules and Ions in Aqueous Media and Biofluids. 122(3), 3459–3636.
- [27] Hajer Hrichi, Nadia, Ali, A.M. and Abdou, A. (2022). A novel colorimetric chemosensor based on 2-[(carbamothioylhydrazono) methyl]phenyl 4-methylbenzenesulfonate (CHMPMBS) for the detection of Cu(II) in aqueous medium. *Research on Chemical Intermediates*, 49(5), 2257–2276.
- [28] Dongare, P.R., Gore, A.H. and Ajalkar, B.D. (2019). A dual colorimetric chemosensor based on Schiff base for highly selective and simultaneous recognition of CN^- and Sn^{2+} . *Inorganica Chimica Acta*, [online] 502, 119372.
- [29] Nural, Y., Keleş, E., Aydiner, B., Seferoğlu, N., Atabey, H. and Seferoğlu, Z. (2021). New naphthoquinone-imidazole hybrids: Synthesis, anion recognition properties, DFT studies and acid dissociation constants. *Journal of Molecular Liquids*, 327, 114855.

- [30] Suguna, S., David, C.I., Prabhu, J. and Nandhakumar, R. (2021). Functionalized graphene oxide materials for the fluorometric sensing of various analytes: a mini review. *Materials Advances*, 2(19), 6197–6212.
- [31] Gerard, T., Wei, Y., Weerawardhana, E., Lugosan, A., Zeller, M., Dickie, D.A., Li, P. and Lee, W.-T. (2023). An Inorganic Fluorescent Chemosensor: Rational Design and Selective Mg^{2+} Detection. *ACS Omega*, 8(4), 3835–3841.
- [32] Ye, X.-L., Li, P., Liu, Y.-L., Liang, X.-M. and Yang, L. (2021). A dual-mode fluorescent probe based on perylene for the detection of Sn^{2+} . *Inorganic Chemistry Communications*, [online] 130, 108739.
- [33] Praikaew, P., Maniam, S., Charoenpanich, A., Sirirak, J., Promarak, V., Langford, S.J. and Wanichacheva, N. (2019). Water-soluble Cu^{2+} -fluorescent sensor based on core-substituted naphthalene diimide and its application in drinking water analysis and live cell imaging. *Journal of Photochemistry and Photobiology A: Chemistry*, [online] 382, 111852.
- [34] Suguna, S., David, C.I., Prabhu, J. and Nandhakumar, R. (2021). Functionalized graphene oxide materials for the fluorometric sensing of various analytes: a mini review. *Materials Advances*, 2(19), 6197–6212.
- [35] Castro-Riquelme, C.L., Ochoa-Terán, A., Roldán-Villegas, I.Y., Trujillo-Navarrete, B., Miranda-Soto, V., Pérez-Sicairos, S., Pina-Luis, G., Reynoso-Soto, E.A., Labastida-Galván, V. and Ordoñez, M. (2021). Versatile optical

response of pyridylalkyl naphthalenediimides in the interaction with metal ions. *Journal of Molecular Structure*, 1236, 130277.

- [36] Yao, Y., Wu, H. and Ping, J. (2019). Simultaneous determination of Cd(II) and Pb(II) ions in honey and milk samples using a single-walled carbon nanohorns modified screen-printed electrochemical sensor. *Food Chemistry*, 274, 8–15.
- [37] Deng, S., Zhang, X., Zhu, Y. and Zhuo, R. (2024). Recent advances in phyto-combined remediation of heavy metal pollution in soil. *Biotechnology advances*, 72, 108337–108337.
- [38] Bakir, E.M., Sayed, A.R. and El-Lateef, H.M.A. (2022). Colorimetric detection of Hg²⁺ ion using fluorescein/thiourea sensor as a receptor in aqueous medium. *Journal of Photochemistry and Photobiology A: Chemistry*, 422, 113569.
- [39] Chen, J., Tao, J., Yu, H.-F., Ma, C.-P., Tan, F. and Wang, X.-C. (2023). Highly selective chemosensor for the sensitive detection of Hg²⁺ in aqueous media and its cell imaging application. *Spectrochimica Acta Part A: Molecular and Biomolecular Spectroscopy*, 296, 122648.
- [40] Halder, S., Roy, S. and Chakraborty, C. (2022). Multicolored and durable electrochromism in water soluble naphthalene and perylene based diimides. *Solar Energy Materials and Solar Cells*, 234, 111429.

- [41] Ghule, N.V., Bhosale, R.S., Puyad, A.L., Bhosale, S.V. and Bhosale, S.V. (2015). Naphthalenediimide amphiphile based colorimetric probe for recognition of Cu^{2+} and Fe^{3+} ions. *Sensors and Actuators B: Chemical*, 227, 7–23.
- [42] Tümay, S.O. and Yeşilot, S. (2023). Synthesis, characterization, and photophysical and fluorescence sensor behaviors of a new water-soluble double-bridged naphthalene diimide appended cyclotriphosphazene. *Turkish Journal of Chemistry*, 47(5), 1296–1306.
- [43] Uzun, D., Ozser, M.E., Kivanc Yuney, Huriye Icil and Demuth, M. (2003). Synthesis and photophysical properties of N,N'-bis(4-cyanophenyl)-3,4,9,10-perylenebis(dicarboximide) and N,N'-bis(4-cyanophenyl)-1,4,5,8-naphthalenediimide. *Journal of Photochemistry and Photobiology A Chemistry*, 156(1-3).
- [44] Asir, S., Demir, A.S. and Icil, H. (2010). The synthesis of novel, unsymmetrically substituted, chiral naphthalene and perylene diimides: Photophysical, electrochemical, chiroptical and intramolecular charge transfer properties. *Dyes and Pigments*, 84(1), 1–13.